GENETIC AND FUNCTIONAL ANALYSIS OF SIDEROPHORES IN TRICHODERMA VIRENS

A Senior Honors Thesis

by

GLORIA VITTONE

Submitted to the Office of Honors Programs
Texas A&M University
In partial fulfillment of the requirements of the

UNIVERSITY UNDERGRADUATE
RESEARCH FELLOWS

April 2008

Major: Biochemistry and Genetics
Minor: Spanish

ABSTRACT

Genetic and Functional Analysis of Siderophores in *Trichoderma virens*

(April 2008)

Gloria Vittone
Department of Biochemistry and Biophysics
Texas A&M University

Fellows Advisor: Dr. Charles Kenerley
Department of Plant Pathology and Microbiology

Trichoderma virens, an avirulent plant symbiotic fungus ubiquitous in soils worldwide, is remarkable as it induces systemic resistance in plants, enhances plant growth, and acts as a mycoparasite of plant-pathogenic fungi. For all microorganisms, the ability to acquire environmental iron is essential for fitness and survival. The ability of *T. virens* to acquire iron from the soil determines its success as a beneficial microorganism for plants and saprophyte of organic material. The most successful strategy developed by microbes for iron acquisition has been the production of siderophores, secondary metabolites that bind iron tightly and are produced in both intracellular and extracellular forms. Extensive genomic analysis of the genome

sequence of *T. virens* revealed the presence of three genes, *Tex10, Tex20,* and *Tex21* that encode siderophore-producing enzymes known as non-ribosomal peptide synthetases (NRPSs), but their regulation and function are largely unknown. To study the function of these secondary metabolites in the life strategy of *T. virens*, two genes encoding the NRPSs for the biosynthesis of siderophores (*Tex10* and *Tex20*) were disrupted by fungal transformation. While the *Tex20* mutants are phenotypically very similar to wild type, the *Tex10* mutant shows some striking differences. Additionally, the *Tex10* mutant shows less ability to respond to oxidative stress. Gene expression of these NRPS-encoding genes was also analyzed in wild type and mutant strains. Siderophore production reaches a maximum at three days in iron depleted medium, while cultures grown in ferrated medium show a dramatic reduction in siderophore production, as well as NRPS gene expression. Correspondingly, several NRPS-encoding gene deletion strains reveal both lower mRNA and siderophore levels. Siderophore production at the peak expression time was corroborated by High Performance Liquid Chromatography. This information is essential for the enhancement of the beneficial capabilities of *T. virens* for global agricultural improvement.

DEDICATION

I would like to dedicate this work to the people who have always encouraged me to achieve my goals and try my hardest. To my future husband, A.J., for his love and support along every step of the way, and to my family, Evelyn, John, and Cynthia, for their love and belief in me throughout my entire life.

ACKNOWLEDGEMENTS

I would like to acknowledge the immense amount of help that my lab-mates have provided me. Without the help and support of Dr. Charles Kenerley (principal investigator), Dr. Prasun Mukherjee, Dr. Walter Vargas, Frankie Crutcher, and Dr. Slavica Djonovic, this project would not have been possible. I have them to thank for a wonderful undergraduate research experience that has inspired me to pursue a life-long career of scientific research.

I am also grateful for the drive and challenge provided by the Department of Honors Programs University Undergraduate Research Fellows Program as well as for provision of the Summer University Undergraduate Research Fellows (SUURF) scholarship.

TABLE OF CONTENTS

LIST OF FIGURES

FIGURE Page

LIST OF TABLES

I INTRODUCTION[1]

The research interest in *Trichoderma virens* that has developed over the past several decades is attributable to its unique and impressive capabilities as a biological control agent, a plant symbiont, and an elicitor of plant systemic resistance (Harman *et al.*, 2004). Biological control, or biocontrol, is the use of a living organism to control another pathogenic organism (Vinale *et al.*, 2008). In this case, *Trichoderma* species can directly parasitize fungal plant pathogens such as *Pythium ultimum* and *Rhizoctonia solani* (Jayaraj & Radhakrishnan, 2008, Lewis *et al.*, 1998, Djonovic *et al.*, 2006, Djonovic *et al.*, 2007). For these reasons research has been directed towards understanding the molecular mechanisms underlying these incredible capabilities with the goal of enhancing them. Incorporating the use of efficacious biocontrol agents into management practices has the potential to insure agricultural success and stability.

There are several characteristics or attributes of microbes that may be targeted for enhanced development. A vital aspect of any microbe's metabolism is the uptake, storage, and utilization of iron (Fe). Many of the physiological aspects of iron's reduction-oxidation (redox) processes remain unclear. It is, however, well known that

[1] This thesis follows the style and format of *Molecular Plant Pathology*.

Fe(II) acts as an electron source for Fe-oxidizing organisms while Fe(III) acts as an electron sink for Fe-reducing organisms (Weber *et al.*, 2006). Fe is also a cofactor for some enzymes and a component of iron-sulfur proteins (such as protein complexes in the mitochondrial electron transport chain). Additionally, Fe is an essential structural component of proteins, such as ferrichrome, that contain metal-liganded domains (R.H. Garrett, 2005).

Soil-dwelling microorganisms must obtain their intracellular Fe from mineral deposits in the soil. As soil exists at circumneutral pH (about 7), Fe in its divalent and trivalent states is largely insoluble, existing mostly as iron hydroxides. As a result, Fe is inaccessible to the internal workings of microorganisms. However, as acidity increases so does Fe(III) solubility (Weber *et al.*, 2006, Winkelmann, 2007). Thus, in order to utilize the insoluble iron sources present in the soil, microbes have evolved a mechanism of uptake and storage that comprises the most efficient and extensive iron-uptake method known today. These microbes produce siderophores, low molecular weight iron-chelating secondary metabolites that can remain intracellular or be secreted into the surroundings (Winkelmann, 2007). Fungi exploit the surrounding soil environment for nutrients primarily by hyphal extension. In this way, fungi secrete siderophores into the

soil to chelate or bind tightly iron that is subsequently brought back into the cell by specific uptake mechanisms. This iron will be used for diverse processes that are essential to the organism's survival (Winkelmann, 2007).

The goal of my Honors University Undergraduate Fellows research was to develop an understanding of the presence, regulation, and function of siderophores in *T. virens*. Research regarding these molecules in fungal biocontrol agents has been meager, yet knowledge of siderophores is vital to the understanding of iron metabolism and its effect on pest management. Iron acquisition can determine survival in competitive environments in that organisms most able to acquire the insoluble Fe from the soil can better compete and survive (Johnson, 2007, Miethke & Marahiel, 2007). In various fungi, siderophore activity has been implicated in many processes other than iron uptake (Schrettl *et al.*, 2007, Wiebe, 2002, Hissen *et al.*, 2004, Lee *et al.*, 2005, Oide *et al.*, 2006). *Trichoderma virens* is a unique fungus whose great potential merits substantial scientific attention. For these reasons, knowledge of siderophores in *T. virens* could reveal connections to its remarkable capabilities such as biological control or plant resistance elicitation. Since iron is involved in this organism's basic metabolism, an enhancement of this uptake could yield a more efficient and productive mutant available

for pest management. These strains of *T. virens* could be more effective biological control agents or resistance elicitors due to enhanced siderophore production or iron acquisition.

II LITEARTURE REVIEW

The Ecology of Iron

As the fourth most abundant element in the earth's crust, iron's biogeochemical functions are being extensively studied. Iron (Fe) is necessary for all organisms and plays an extensive role in microbial metabolism as it is required for many cofactors of various metabolic processes (Haas, 2003). For this reason, the metabolic activities of microorganisms dictate the reduction/oxidation (redox) chemistry in most environments on earth. Iron exists primarily in two insoluble states [ferrous: Fe(II) and ferric: Fe(III)] at circumneutral pH (approximately pH 7), and its solubility increases with decreasing pH. However, in aerobic environments, oxygen reacts with Fe(III), forming ferric hydroxides which are insoluble (Johnson, 2007). Microbes have adapted to use iron as both an electron donor and acceptor in various metabolic processes. As an electron donor, lithotrophic iron-oxidizing microorganisms utilize Fe (II) aerobically and anaerobically during the breakdown of organic molecules. As an electron acceptor, Fe(III) can be utilized anaerobically by lithotrophic and heterotrophic iron-reducing microorganisms. This dynamic environmental redox cycle is established by the interplay of various microorganisms such as bacteria, fungi, and archaebacteria. The vital role

these organisms play in the dynamics of soil environments has been extensively studied such as their application in remediation of acid mine drainage via iron absorption (Weber et al., 2006, Baker & Banfield, 2003). Additionally, microbial reduction of Fe(II) yields biogenic magnetite which is responsible for the natural magnetization of deep sea sediments (Chaudhuri *et al.*, 2001). These and many other ecological parameters are impacted by iron-metabolizing microbes in soil environments (Weber *et al.*, 2006).

Iron is not only used in microbial redox reactions and electron transport mechanisms; it also interacts with various transcriptional and posttranscriptional regulators to control gene expression involved in iron acquisition and protection from reactive oxygen species. Furthermore, it has been shown that a large proportion of some proteomes consists of proteins that require iron both structurally and functionally (Miethke & Marahiel, 2007). Although iron is abundant in soil environments, it exists, as mentioned above, primarily in an insoluble state. Bioavailable iron exists in soil only at about 10^{-18} molar (Neilands JB & A, 1987). Thus, microbes have been forced to develop unique mechanisms for acquisition and use of iron sources such as the production of high-affinity iron-chelators that can accept and solubilize a variety of iron sources.

Iron Acquisition via Siderophores

Non-ribosomal peptide synthetases (NRPS) are encoded by multi-gene clusters and are responsible for the synthesis of numerous biologically important compounds such as antibiotics and peptaibols (Wiest *et al.*, 2002, Grunewald & Marahiel, 2006, Finking & Marahiel, 2004). Most antibiotics are produced non-ribosomally by bacteria and have distinguishing chemical modification such as fatty acid chains which are components of fengicin and surfactin (Finking & Marahiel, 2004). Peptaibols are short, linear peptides usually containing an acetyl group at the N-terminus and an amino-alcohol group at the C-terminus. They exhibit antimicrobial activity due to their ability to modify cell membranes of phytopathogenic bacteria and fungi (Wiest *et al.*, 2002). In addition to the bioactive peptaibols, other secondary metabolites such as gliotoxin and gliovirin have been implicated in prevention of damping-off in plants caused by *Pythium ultimum* (Wilhite *et al.*, 2001).These secondary metabolites (peptaibols, antibiotics) along with ribosomally-produced cell wall degrading enzymes such as glucanases and chitinases established *T. virens* as an effective mycoparasite (Wiest *et al.*, 2002).

NRPSs were discovered in a 1960's experiment in which these peptides were produced despite repression of the ribosomal machinery (Finking & Marahiel, 2004). NRPSs generally consist of three discrete domains: adenylation (or AMP-binding), condensation, and peptidyl carrier protein (PCP or thiolation). These act together to incorporate an individual amino acid into the developing polypeptide and exist in various combinations to produce a multitude of variable products (Finking & Marahiel, 2004). These domains cooperate to recognize, activate, and incorporate amino acid subunits in a polypeptide chain by the binding of amino acids to PCPs and peptide bond formation by condensation domains (Stack *et al.*, 2007). The amino acid is first recognized and activated by the adenylation domain, bound to a 4'phosphopantetheine (PP) cofactor in the thiolation domain, and added to the growing chain via peptide bond formation by the condensation domain (Johnson, 2007). However, the number of modules and the number of amino acids are not always in a 1:1 ratio. Adenylation domains from the modules can be use repeatedly if extra PCP and condensation domains are present (Johnson, 2007). The amino acids in the growing chain can also be chemically modified by tailoring regions. A cyclization event catalyzed by a thioesterase domain usually releases the chain from the NRPS. Type II thioesterases perform trans-

editing by catalyzing the de-acylation of mis-acylated regions (Miethke & Marahiel, 2007). The gene cluster that encodes an NRPS gene can encode NRPS-modifying enzymes: the action of the cluster as a whole produces a unique biological compound (Llewellyn & Spencer, 2007).

One of the primary products of NRPS enzymes is a class of low molecular weight iron-chelators termed siderophores. These comprise the most pervasive and successful system for microbiological acquisition of iron. The biosynthetic pathways which NRPSs catalyze for siderophore synthesis have been extensively studied, especially in the bacterial community (Miethke & Marahiel, 2007). Siderophores show extremely high affinity for ferric iron, Fe(III), and come in approximately 150 structurally different forms (Winkelmann, 2007). The major classes of these hydroxamate compounds are ferrichromes, coprogens, and fusarinines. Three hydroxamate groups are linked by a NRPS and sometimes combined with other amino acids to form the final siderophore (Fig. 1, Johnson, 2007).

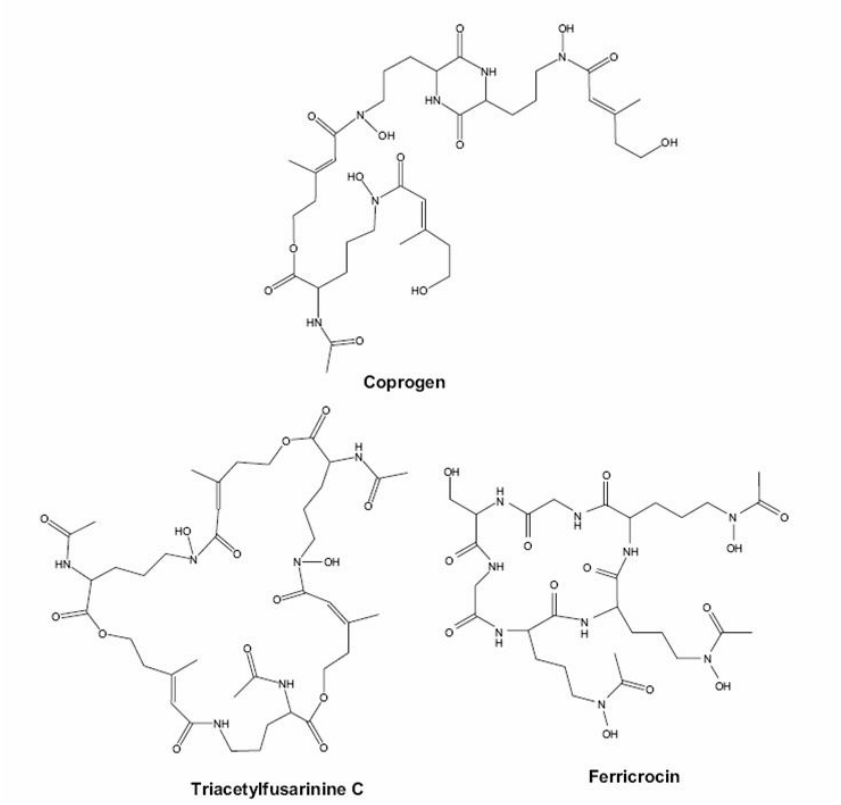

Fig. 1 Representative siderophore structures (Johnson, 2007).

Organisms tend to secrete siderophores from each class to accommodate a broad range of environmental situations (Johnson, 2007). Siderophores have also been encountered as both intracellular and extracellular compounds in various fungi and bacteria. Intracellular siderophores are primarily used to store Fe and the primary fungal intracellular siderophore is ferricrocin, which has been shown to be involved in sensitivity to oxidative stress (Johnson, 2007). Siderophore secretion, as thus far

understood in a few microbes, occurs through efflux pumps of the major facilitator superfamily (MFS) which are also responsible for re-absorption of iron-charged siderophores (Miethke & Marahiel, 2007). Once the siderophore has acquired a Fe (III) ion, there are two pathways of iron uptake: (i) membrane-bound ferrisiderophore reductases receive the ferric ion from the siderophore and pass it through the membrane, or (ii) the whole ferrisiderophore complex can be imported to the cytoplasm. Two general methods also exist for the release of iron from the siderophore: (i) Fe(III) is first reduced to Fe(II) which is spontaneously released from the siderophore, or (ii) hydrolysis of the ferrisiderophore complex lowers its stability thus releasing Fe(III) which will be subsequently reduced or bound to intracellular Fe-binding compounds (Miethke & Marahiel, 2007). Since microbial iron oxidation has a large impact on soil ecology, the genetic regulation of siderophore activity has attracted much attention and occurs mostly at the transcriptional level (Miethke & Marahiel, 2007). Iron acts as a regulatory signal for genes involved in siderophore synthesis and action. Therefore, depending on the amount of iron in the surrounding environment, gene expression must be modified which in turn activates or deactivates siderophore biosynthesis pathways (Johnson, 2007). Various bacteria regulate iron metabolism with ferric uptake regulation

(Fur) proteins which show transcriptional repression in ferric environments. The binding of iron to the Fur protein inhibits the access of RNA polymerase to the promoter region of iron regulation genes (Winkelmann, 2007). Although siderophores appear to be a purely advantageous evolutionary advancement, they do come with a cost. The ATP requirement of siderophore production is significant, thus disallowing organisms the ability to constitutively produce them. An organism that often produces siderophores may be less competitive for nutrients in natural ecosystems (Winkelmann, 2007).

Studies of Fungal Siderophores

Studies of the production, regulation, and function of fungal siderophores are essential for understanding the survival and proliferation of these organisms in soil environments. Many groups have discovered the roles of these siderophores by creating a mutant strain deficient in the NRPS-encoding gene that synthesizes the siderophore (Johnson, 2007). Several studies have demonstrated that siderophores are involved in processes beyond the acquisition and storage of iron (Lee *et al.*, 2005, Oide *et al.*, 2007, Oide *et al.*, 2006, Schrettl *et al.*, 2007, Johnson, 2007). However, the diverse functions of siderophores in fungi used for biological control have yet to be studied in depth. Fungi primarily use extracellular siderophores for scavenging iron in conditions of iron

deprivation while intracellular siderophores act in iron storage. While molecular studies of siderophores were initiated in the plant pathogen *Ustilago maydis*, more modern regulatory and functional studies have used *Aspergillus nidulans* or *Neurospora crassa*, two well developed model systems representing non-pathogenic eukaryotes(Haas, 2003). Studies have revealed that revealed that mechanisms for extraction of iron from siderophores in cells are diverse (Haas, 2003). More recent studies have focused on other functions of siderophores and their genetic regulation. The effect of environmental conditions on siderophore production was demonstrated in chemo-stat studies. These showed that in iron-free conditions, the growth rate of *Fusarium venenatum* A3/5 was reduced by nearly 50%, but the concentration of siderophores per unit of biomass nearly doubled. It was also illustrated that the optimal pH for siderophore production is 4.7 (Wiebe, 2002). Studies in the fungal mammalian pathogen, *Aspergillus fumigatus*, revealed the major siderophores are triacetylfusarinine C (TAFC) and ferricrocin have high iron affinity (Hissen et al., 2004). Later, it was found that intercellular ferricrocin is responsible for hyphal iron storage, and that the removal of iron from transferrin via these siderophores is vital for this pathogen's survival in human serum (Hissen *et al.*, 2004). The likely genes involved in the biosynthesis of these siderophores were later

identified as three NRPS-encoding genes: sidC, sidD, and sidE (Reiber *et al.*, 2005). Iron-depleted conditions were again tested and shown to increase sidD and sidC expression up to 90%. A proposed biochemical pathway for siderophore synthesis in this fungus includes five "sid" genes that catalyze the formation of four siderophores, the fourth being hydroxyferricrocin (Schrettl *et al.*, 2007). All five mRNA transcripts are dramatically overproduced under iron starvation while basal levels are negligible (with sufficient iron). Two of these genes were also implicated in the detoxification of hydrogen peroxide. In addition, virulence correlates with a pathogen's ability to acquire iron from its host. The correlation between siderophore gene expression and virulence was demonstrated in a murine host. A mortality rate of 100% was observed in mice infected with wild-type *A. fumigatus,* while mice infected with ΔsidC or ΔsidF resulted in only 41% and 36% mortality, respectively (Schrettl *et al.*, 2007).

The recent availability of various fungal genome sequences has accelerated progress in the identification of siderophores in fungi. A total of 12 NRPS genes were found in the *Cochliobus heterostrophus* genome suggesting that some of these are responsible for siderophore production. A homolog of SidD, termed NPS6, has been shown to be involved in a variety of processes in the plant pathogenic fungi,

Cochliobolus miyabeanus and *C. heterostrophus* (Stack *et al.*, 2007). NPS6 has been shown to be involved in virulence and oxidative stress protection as well as sensitivity to iron starvation. Specifically, deletion of NPS6 caused reduced maize virulence and increased sensitivity to hydrogen peroxide (Oide *et al.*, 2006) . In general, sensitivity to oxidative stress increases with siderophore inactivity because enzymes such as catalases that breakdown reactive oxygen species require a heme cofactor. The inability to acquire iron renders catalases ineffective against species such as hydrogen peroxide. One of these twelve genes, NPS2, was later shown to be involved in sexual development via ascus/ascospore formation. NPS2 is responsible for ferricrocin biosynthesis intracellularly (Oide *et al.*, 2007). Therefore, the interplay between iron and siderophores is essential for sexual development in these fungi, though the exact molecular mechanisms are yet to be elucidated.

Additionally, analysis of gene clusters has led to the discovery of genes that encoding siderophore-producing NRPSs. *Omphalotus olearius* was shown to produce ferrichrome A under iron starvation via the up-regulation of *fso1* (which encodes a NRPS). Interestingly, fso1 encodes a NRPS enzyme similar in structure to those of the homologous genes in *U. maydis* and *A. nidulans* (Welzel *et al.*, 2005). This was the first

siderophore gene cluster found to be under iron regulation and is under transcriptional control of GATA factors Urbs1 and SREA (Welzel *et al.*, 2005). Bioinformatics allowed for the identification of 15 NRPS genes in *Fusarium graminearum* and the NPS2 gene was found to code for ferricrocin biosynthesis (Tobiasen *et al.*, 2007). It is undeniable that biological research is tending toward the analysis of questions that are generated through bioinformatic analyses.

Siderophores in *Trichoderma virens*

Biological control agents are widespread, especially in the bacterial community, and siderophore activity in these biocontrol agents has received much attention (Mercado-Blanco & Bakker, 2007). However, the roles and interactions of siderophores in fungal biocontrol agents have yet to be explored. *T. virens* is a plant symbiotic, avirulent fungus whose capabilities for biological control have been genetically enhanced (Harman *et al.*, 2004). Not only does it show mycoparasitic ability, but can also induce systemic resistance in plants and enhance plant growth and development (Harman *et al.*, 2004). NRPS genes in *T. virens* have been demonstrated to produce antimicrobial compounds such as peptaibols (Wiest *et al.*, 2002, Wei *et al.*, 2005). However, iron uptake mechanisms and their regulation in this fungus have been studied

to a very limited extent. *Trichoderma virens* (teleomorph *Hypocrea virens*) showed restricted growth (only ~84 mg/L of biomass) in an iron-deficient medium. However, small amounts of iron (3 mg Fe/L) increased biomass production to as much as 215 mg/L. Biomass did not increase significantly with ten and twenty times more iron in the medium (Jackson *et al.*, 1991). The major siderophores in culture filtrates of *T. virens* were cis- and trans-fusarinine (cF, tF) and dimerum acid (DA) along with minor amounts of several trihydroxymates (coprogen, coprogen B, and ferricrocin) (Jalal *et al.*, 1986). At pH 6.5-8, the fusaranines existed as 3:1 chelates with Fe (i.e., $Fe(cF)_3$) and dimerum acid exists as a 3:2 chelate.

Siderophore production was shown to reach a maximum (~0.7g/L), along with fungal biomass, at approximately 10 days. Of the total siderophores produced, DA comprised 45%, cF 23%, and tF 22% (Jalal *et al.*, 1986). A time course study of iron uptake by these three siderophores showed an exponential increase in siderophore production which begins to reach an asymptote at about 15 minutes after iron was added. It was also shown that other fungal species could utilize these siderophores to uptake iron for themselves (Jalal *et al.*, 1987). Although secondary metabolites such as peptaibols and cell wall degrading enzymes have been studied thoroughly in *T. virens*,

siderophores have yet to be analyzed beyond their general presence (Djonovic *et al.*, 2006, Wiest *et al.*, 2002, Wei *et al.*, 2005, Djonovic *et al.*, 2007). Therefore, research into the regulation and function of siderophores is vital to provide an understanding of iron metabolism and its possible role in other life processes in biocontrol agents.

III EXPERIMENTAL PROCEDURES

Vector Construction for NRPS Gene Disruption

The genome sequence of *Trichoderma virens* was published by the Joint Genome Institute (JGI) in the summer of 2007 (http://genome.jgi-psf.org/Trive1/Trive1.info.html), allowing intensive bioinformatic analysis of sequences encoding potential NRPSs. Thirty-two NRPSs from the JGI sites (based on the presence of adenylation and condensation domains) were analyzed by BLASTP (Basic Local Alignment Search Tool, Proteins) to elucidate the organization of the NRPS domains. Of these genes, homology to NRPSs in other fungi was determined using BLASTP. Based on this homology, three genes encoding NRPS enzymes which produce siderophores were identified in this genome (Dr. Prasun Mukherjee, unpublished data): *Tex10*, *Tex20*, and *Tex21*.

A functional genomics approach was taken to determine the role siderophores in *T. virens.* The initial goal was to generate a vector that would be used to disrupt a sufficient coding region of the targeted gene, *Tex21* resulting in a mutant unable to produce the targeted siderophore. This was done using the principles of homologous recombination to replace the central portion of the gene with a selectable marker for

antibiotic resistance. The mutants could then be grown in medium amended with that antibiotic so that only cells that incorporated the deletion construct into the genome survive.

Double-joint (DJ) polymerase chain reaction (PCR) was the method used to create the gene deletion construct (Yu *et al.*, 2004). This method consists of three main steps: (i) amplification of the left, right, and central flanks separately (Fig. 2A), (ii) fusion of the three flanks via DJ-PCR (Fig. 2B), and (iii) nested PCR to amplify large amounts of the entire construct (Fig. 2C). The left and right flanks consist of regions on the left and right side of the normal gene. The central flank is the hygromycin resistance marker (Hyg) which consists of the TrpC promoter and the Hph (hygromycin phosphohydrolase) open reading frame (ORF). Wild type *Trichoderma virens* does not normally encode genes for hygromycin resistance; therefore by inserting this gene into the chromosome to generate mutants, survival in medium amended with hygromycin is possible.

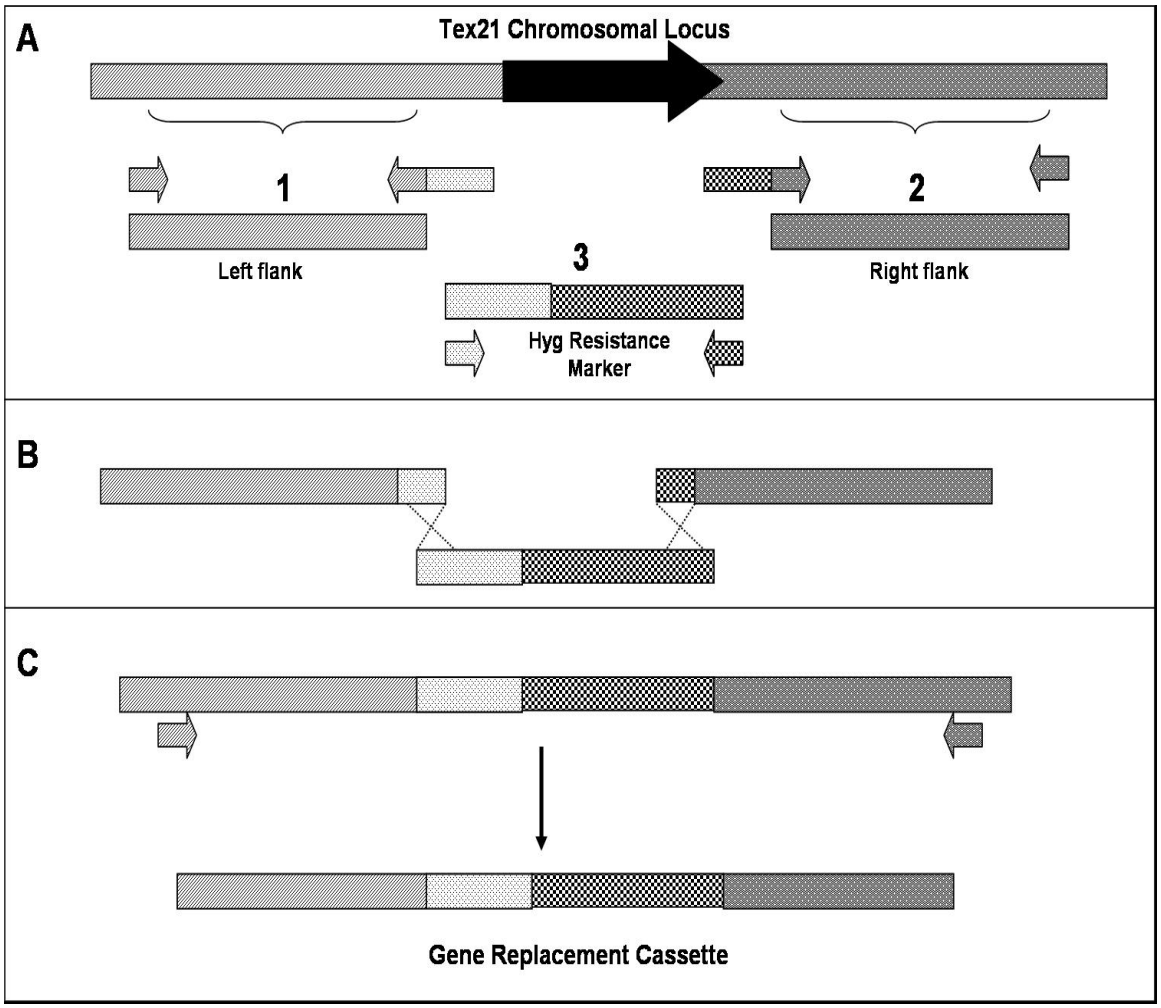

Fig. 2 Schematic representation of the DJ-PCR process. This was used to create a *Tex21* gene replacement cassette. (A) Each of the three segments is amplified separately. The left and right flanks have primers that anneal to the left and right regions of the *Tex21* chromosomal locus. These primers also have tails that are homologous to the ends of the Hyg fragment (B) The three fragments are combined for the double joint PCR reaction in which the tails that were added onto the left and right flanks by the primers from part A will anneal to the ends of the Hyg segment. (C) The product of the previous reaction will be used with nested primers to amplify the major portion of the cassette that will be introduced into cells to replace the chromosomal locus. The small arrows represent primers whose sequences are provided in Table 1.

The central region of the gene will be deleted because the flanks in the construct will be homologous to the left and right regions of the gene in the genome. Therefore, a double crossover will occur and replace this central portion of the gene with the resistance marker chosen (Fig. 3).

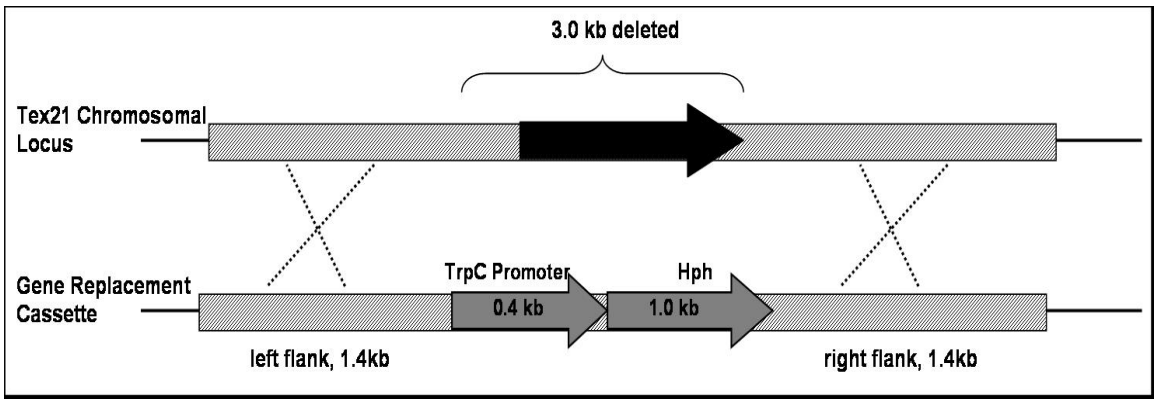

Fig. 3 *Tex21* gene deletion scheme. The gene replacement cassette (Fig. 2) will recombine with the chromosomal locus to replace the central portion of the locus with the Hyg resistance marker (comprised of the TrpC promoter and Hph). The arrows indicate ORFs.

The primer sequences and their role in vector construction are presented in Table 1. The first step in the DJ-PCR process is to amplify all three flanks separately by PCR using the primer pairs indicated in Table 1. A GeneAmp PCR System 9700 (Applied Biosystems) thermocycler machine was used for all PCR reactions. All primers were

obtained from the Gene Technologies Laboratory (GTL) at Texas A&M University. For the amplification of the flanking regions, the follow parameters were used: 96˚C priming for 3 min, 35 cycles of (i) 94˚C strand separation for 30 seconds, (ii) 54˚C annealing for 30 seconds, and (iii) 72˚C elongation for 2 minutes, a holding period of 10 minutes at 72˚C, and a final hold at 4˚C. The PCR reaction mix is presented in Table 2. The resultant DNA was purified by precipitation with 1/10 volume of sodium acetate and 2 volumes of 95% ethanol. The purified product was placed at -80˚C for 30 minutes, washed with ethanol, then pelleted by centrifugation at 13,000 rpm. The quality of each amplified flank was assessed by electrophoresis in a 1% agarose gel stained with ethidium bromide.

Table 1 Primer sequences and role in the generation of the *Tex21* gene disruption cassette.

Primer	Sequence (5' – 3')	T_m (˚C)	Usage
*Tex21*LFs	TTACGACACCATCAAATCACGT	54.5	Left flank
*Tex21*LFas	ATTGATGTGTTGACCTCCAAT GTGCTGAAGAGTCACGAATGCT	n/a	Left flank (+ tail)
*Tex21*RFas	ATTCATTCTCGAATAGCTTGGCA	54.6	Right flank
*Tex21*RFs	TCTGGATATAAGATCGTTGTT GTCTCAGTTGGCCGATTCGACTT	n/a	Right flank (+ tail)
*Tex21*nestF	AGAGTTGAAGAAGCCAACGG	55.2	Nested PCR
*Tex21*nestR	GTTGTCGTGAACAAAGGCTTG	54.9	Nested PCR
HygF	GTGGAGGTCAACACATCAAT	53.0	Hyg fragment
HygR	GACACCAACGATCTTATATCCAGA	54.0	Hyg fragment

Abbreviations: LF (left flank), s (sense), as (antisense), RF (right flank), F (forward), R (reverse), nest (used for nested PCR), Hyg (hygromycin).

Table 2 Components of the PCR reactions used to amplify separately the left, right, and hygromycin flanks.

Component	Volume per reaction (µL)
10X Buffer (ThermoPol)	5.0
2.5 mM dNTP mix	4.0
Taq DNA Polymerase	0.5
Distilled H_2O	37.5
10nM Primers (forward and reverse)	1.0
DNA template sample	1.0
Total Per Reaction	**50**

The double joint PCR was conducted without primers, since the two central primers of the left and right flanks include a “tail” which is homologous to regions in the Hyg flank (Fig. 2). Thus, these ends will be the glue that brings the three pieces of the construct together as one. For a DJ reaction, 100 ng of left flank DNA, 300 ng Hyg DNA, and 100 ng of right flank DNA are used along with 2 µL of dNTP mix, 2.5 µL ThermoPol buffer (New England BioLabs), and 0.25 µL Taq DNA Polymerase. The reaction volume is filled to 25 µL with water. The thermocycler was used for the double joint reaction (in which all three flanks will be fused) with these parameters: 94˚C priming for 2 min, 15 cycles of (i) 94˚C strand separation for 30 seconds, (ii) 55˚C annealing for 20 minutes, and (iii) 72˚C elongation for 7 minutes, a holding period of 10 minutes at 72˚C, and a final hold at 4˚C.

The DJ-PCR product served as the template DNA for the nested PCR reaction in which primers that begin just inside the ends of the left and right flanks are used to amplify a desired amount of the final construct which would yield the final gene disruption cassette (Fig. 2). The components used for the nested PCR reaction are listed in Table 3 and the thermocycler parameters were: 96˚C priming for 3 min, 35 cycles of (i) 94˚C strand separation for 30 seconds, (ii) 55˚C annealing for 30 seconds, and (iii)

72˚C elongation for 5 minutes, a holding period of 10 minutes at 72˚C, and a final hold at 4˚C. The DNA precipitation protocol listed above was preformed with this PCR product to yield the vector used in the transformation protocol below.

Table 3 Components of the nested PCR reaction.

Component	Volume per reaction (µL)
10X Buffer (ThermoPol)	5.0
2.5 mM dNTP mix	4.0
Taq DNA Polymerase	0.5
Distilled H_2O	36.0
10nM Primers (Nest forward and reverse)	2.0
DJ product template	0.5
Total Per Reaction	**50**

The primer sequences are listed in Table 1.

A similar protocol was used to generate a deletion cassette for *Tex10* (Fig. 4), a gene which encodes a NRPS which produces the siderophore ferricrocin in *F. graminearum* (Dr. Prasun Mukherjee, unpublished data) as well as for *Tex20*, a NRPS-encoding gene which produces the siderophore TAFC in *Aspergillus fumigatus* (Darlene Grzegorski, unpublished data), so as to analyze the role of each of the three siderophores in *T. virens*.

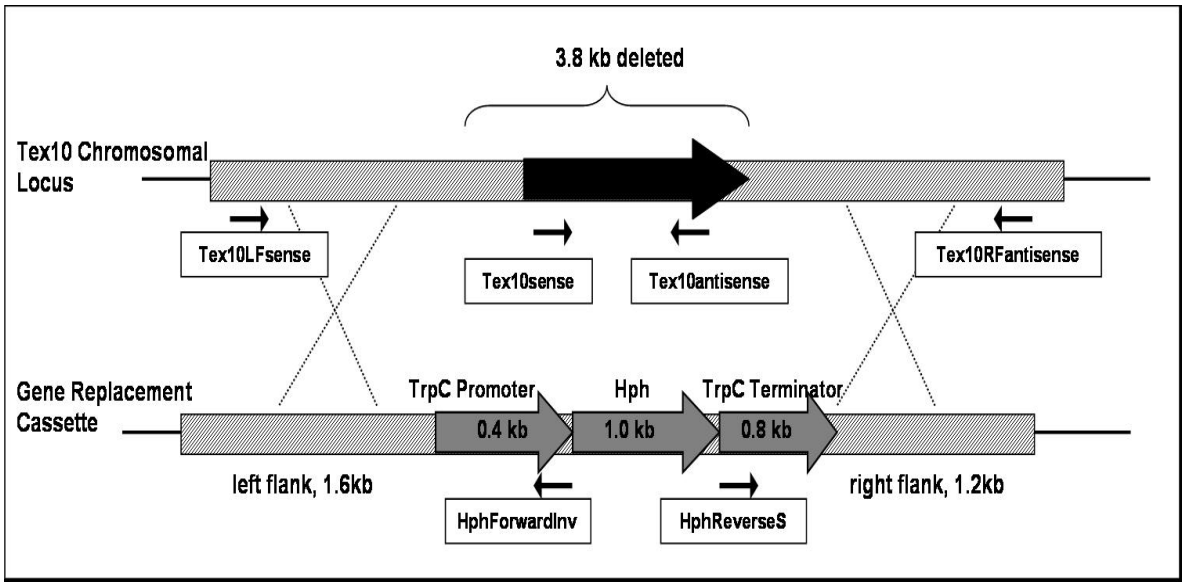

Fig. 4 *Tex10* deletion scheme and primer positions for knockout verification. The large arrows indicate ORFs. The small black arrows indicate primer positions and are indicated with names that correspond to Table 4 (below).

The deletion scheme for *Tex20* was unique in that it was achieved by complementing an auxotroph. *T. virens* strain 10.4 is deficient in ARG2, which encodes the amino acid arginine (Baek & Kenerley, 1998). This strain cannot grow under normal conditions. Therefore, the selectable marker used in this strain was ARG2. In this way, replacement of the *Tex20* gene with a cassette that contains ARG2 would restore the ability of this strain to produce arginine and thus survive. Additionally, the ARG2 ORF in the *Tex20* deletion cassette is reversed compared to the Hyg ORFs in the *Tex10* and *Tex21* cassettes.

Transformation of *T. virens*

Transformation is a polyethylene glycol (PEG) mediated process in which the vector is inserted into the genome of *T. virens* protoplasts. When homologous recombination between the vector and the target genome sequence occurs, the central segment of the gene will be replaced by the vector. Protoplasts, cells with the cell wall removed, are generated to facilitate the uptake the vector. Potato Dextrose Broth is inoculated with conidia [harvested from a 7 to12 day-old culture grown on Potato Dextrose Agar (PDA)] at a concentration of approximately 10^8 conidia/mL of broth. Cultures are incubated in 100 mL of Potato Dextrose Broth (PDB) at room temperature for 14-16 hours while shaking at 150 rotations per minute (rpm). After the incubation period, the fungal biomass is harvested on sterile Miracloth and rinsed with 250 mL of sterile water. To prepare the enzyme solution that will digest the cell walls to form protoplasts, 2.0 mg of chitinase, 7.0 mg of lyticase, and 44.0 mg of cellulase are added to 2.40 mL of mannitol osmoticum (50 mM $CaCl_2$, 0.5 mM mannitol, 50 mM N - morpholino ethanesulphonic acid at pH 5.5 with KOH). This suspension is vortexed well, aliquoted evenly into three 1.5 mL epindorf tubes, and centrifuged for 25 seconds at 14,000 rpm. The supernatant of each tube is filter sterilized with a 0.22 micrometer

(μm) filter attachment on a 3.0 mL syringe. This enzyme solution is added to 0.5 g of harvested fungal biomass, and the suspension shaken at room temperature for 25 minutes at 225 rpm. The suspension is then evaluated for the appearance of protoplasts with a hemacytometer. Approximately 10^7 protoplasts per mL are desired for the transformation procedure.

The protoplasts are collected by filtration of the above mixture through a Swinnex filter apparatus equipped with a 10 μm nylon filter membrane attached to a 10 mL syringe. The filtrate is placed in a sterile centrifuge tube and about 2 volumes of mannitol osmoticum are added. This suspension is centrifuged in a Sorvall RC-5B Refrigerated Superspeed Centrifuge in a SM24 rotor (DuPont Instruments) at 5,500 rpm for 10 minutes. The supernatant is carefully discarded and the pellet is resuspended in 200 μL of fresh mannitol osmoticum. To introduce the vector, 240 μL of the protoplast suspension are added to 20 μL of construct DNA (this should be about 10 μg of DNA). As a positive control, 240 μL of protoplasts are added to 60 μL of osmoticum. This is incubated on ice for 20 minutes with gentle mixing every 5 minutes. Next, 130 μL of PEG solution (40% PEG 8000 in mannitol osmoticum) is added to the sample and mixed gently. A second volume of PEG (130 μL) is added and mixed gently. The solution is

incubated for 30 minutes at room temperature and then added to 200 mL of liquefied PDA-Sucrose (PDAS, 0.5 M sucrose in PDA) at 47˚C, mixed thoroughly, and finally aliquoted in portions of 20 mL to plastic petri plates. These plates are incubated at 27˚C overnight. The following day (approximately 14-16 hours later) an overlay (10ml/plate) of hygromycin agar (PDA supplemented with 50 mg/L of hygromycin) is added to each plate to select for protoplasts that have the vector containing the hygromycin resistance marker integrated into the genome. Developing colonies on the hygromycin agar are transferred to hygromycin agar tube slants for further characterization. To purify the colonies of any wild-type cells, conidia from sporulating cultures are transferred several times to fresh hygromycin agar.

Verification of Mutant Strains

Verification of vector integration in hygromycin-resistant isolates was by performed on a *Tex10* isolate (#19) by amplifying a portion of the vector (Fig. 4). DNA was obtained from cultures of the mutant and wild type isolates grown in 100 mL of PDB amended with 50 mg/L hygromycin for 5 days shaking at 125 rpm at room temperature. The mycelium was harvested on Miracloth and rinsed with 100 mL of distilled water. The harvested fungal biomass material was ground in liquid nitrogen,

added (~200 mg) to 500 µL of DNA extraction buffer (100 mM Tris, 50 mM ethylenediaminetetraacetic acid/EDTA, 500 mM NaCl), vortexed, gently mixed with 70 µL of 10% sodium dodecyl sulfate (SDS), and incubated at 65˚C for 10 minutes. Next, 170 µL of ice-cold 3M potassium acetate (CH_3COOK) is added to the suspension, mixed gently, incubated for 20 minutes on ice , and then 500 µL of chloroform (CH_3Cl) are added. This mixture was centrifuged at 13,000 rpm for 10 minutes and the upper (aqueous) phase (~ 500 µL) is retained. The supernatant was added to 0.7 volumes of isopropanol, mixed gently, centrifuged 5 minutes at 13,000 rpm, and the pellet then washed with 200 µL of 80% ethanol (which must be added without disturbing the pellet). The washed pellet was further concentrated by centrifuging for ten minutes at 13,000 rpm. The alcohol was removed and the pellet was dried at room temperature, and then resuspended in 100 µL of water.

For PCR amplification of the selected target sequence, the reaction mix consisted of: 2.5 µL of 10X ThermoPol Buffer (New England BioLabs), 2 µL of 2.5 mM dNTP mix, 0.25 µL of Taq DNA Polymerase (New England BioLabs), 17.25 µL of water, 1µL of each 1X primer, and 1 µL of the extracted DNA sample. The reaction parameters included: 94˚C priming for 2 min, 30 cycles of (i) 94˚C strand separation for 30 seconds,

(ii) 55˚C annealing for 30 seconds, and (iii) 72˚C elongation for 2 minutes, a holding period of 10 minutes at 72˚C, and a final hold at 4˚C. The primer sequences and melting temperatures (T_m) are given in Table 4 and the primer positions are in Fig. 4.

Table 4 Primer sequences used to determine successful insertion of the deletion cassette into the chromosomal locus.

Primer	**Sequence (5' – 3')**	**T_m (˚C)**
*Tex10*LFsense	CTGACTTATCTGTGCTTAACCCA	54.5
HphForwardInv	GCACGAGATTCTTCGCCCTC	58.3
HphReverseS	GATGGACGACACCGTCAGTG	57.9
*Tex10*RFantisense	CGATCTGAGCCGATATCTCCT	55.6
*Tex10*sense	CAAGACGCGTTTCACCTTCTTG	56.7
*Tex10*antisense	CGC TGT CCA TTT GAT CTC GC	56.5

The *Tex10*sense and *Tex10*antisense primers amplify a portion of the deleted ferricrocin gene. Abbreviations: LF (left flank), RF (right flank).

NRPS Gene Expression Analysis

In order to observe the expression pattern of the three NRPS genes in *T. virens,* reverse transcriptase PCR (RT-PCR) was conducted. Reverse transcriptase is an enzyme that translates messenger RNA (mRNA) into cDNA. The overall process is to extract mRNA from fungal cells grown under specific experimental conditions, clean the RNA of any DNA contaminants, perform the RT reaction with the RNA template to generate

cDNA, and conduct a PCR reaction of the cDNA to test for the presence and level of a certain region of the gene.

Siderophores are known to be produced under conditions of Fe deprivation, so a time point experiment was conducted to test for NRPS gene expression in wild type *T. virens* at 3, 5, 7, and 9 days in medium with or without Fe. Fe-free medium required Fe-free glassware and Fe-free water. To make Fe-free glassware, it was first rinsed in tap water, soaked in 0.1% SDS for at least 6 hours, transferred to 0.01% EDTA for 12 hours, and then rinsed in 1% HCl followed by six rinses in twice-distilled water. The glassware was then dried at 160˚C. The medium used to grow the fungal cultures was similar to Grimm-Allen medium (Table 5, (Wilhite *et al.*, 2001). The cultures were grown in 100 mL of this liquid medium in 250 mL Erlenmeyer flasks for 3, 5, 7, and 9 days shaking at 125 rpm at room temperature. These cultures were inoculated with conidia scraped from 7 day-old Grimm-Allen solid agar plates (Fe-free). The spores were washed with distilled water by three repetitions of vortexing and centrifugation. The liquid medium was inoculated with 10^7 conidia quantified by counting with a hemacytometer.

Table 5 Recipes for Grimm-Allen medium and Srb's micronutrient solution (Sanderson & Srb, 1965).

Grimm-Allen Medium		Srb's Micronutrients (300 mL)	
Compound	**Concentration (g/L)**	**Compound**	**Amount (mg)**
K_2SO_4	1	H_3BO_3	9.0
K_2HPO_4	1	$CuSO_4 \cdot 5H_2O$	58.5
$NH_4C_2H_3O_2$	3	KI	1.95
Citric Acid	1	$MnSO_4 \cdot H_2O$	9.0
$ZnSO_4 \cdot 7H_2O$	0.002	$NaMoO_4$	7.6
$MgSO_4 \cdot 7H_2O$	0.08	$ZnSO_4 \cdot 6H_2O$	822.0
Sucrose	20	$FeCl_3 \cdot 6H_2O$	139.8

The Grimm-Allen medium consists of the above components plus 1 ml/L of Srb's micronutrients. The pH was adjusted to 6.8 with NH_4OH. For growth with Fe, 55.6 mg/L of $FeSO_4 \cdot 7H_2O$ were added to the medium. For Fe-free conditions, no $FeSO_4 \cdot 7H_2O$ was added and the ferric chloride was left out of the Srb's micronutrients. When solid medium was needed, 15 g of agar per liter was added.

Fungal biomass was collected at each time point by harvesting the mycelia on Miracloth and washing with 250 mL of distilled water. The culture filtrate was retained and frozen at -80˚C for High Performance Liquid Chromatography (HPLC) analysis. The fungal material was stored at -80˚C until used. To prepare the biomass for RNA extraction, it was frozen in liquid N_2 and ground to homogenization with a mortar and pestle. About 100 mg of this ground tissue was used per RNA extraction (Molecular Research Center, Inc.). The tissue was added to 1 mL of TRI Reagent®, incubated for 10

minutes at room temperature, 0.2 mL of chloroform was added followed by vortexing for 15 seconds, and then incubated at room temperature for 15 minutes. The samples were then centrifuged at 17,000 G for 15 minutes at 4˚C. At this point, the RNA (in the upper, aqueous phase) was transferred to a fresh tube containing 0.5 mL of isopropanol. This solution was incubated for 15 minutes at room temperature and then centrifuged at 12,000 G for 8 minutes at 10˚C. The supernatant was removed and discarded. The pellet was then vortexed with 1 mL of 75% ethanol, and centrifuged at 7,500 G for 5 minutes at 10˚C. The ethanol was removed, the pellet was air dried for about 5 minutes, and resuspended in 15 µL of diethylpropylcarbonate (DEPC), water treated to have no RNases.

The RNA samples were quantified with a NanoDrop (NanoDrop Technologies, Inc.) which was calibrated with DEPC water. The quality of the RNA sample was determined by electrophoresis in a 1% agarose gel with 5 µL of the RNA sample and 1 µL of 6X blue/orange loading dye (Promega) per well. A 1 Kilobase (kb) Plus DNA Ladder (1µg/µL, Invitrogen) was used as a molecular weight standard.

The RNA sample was treated with a DNase cleaning kit (Ambion) to remove DNA contaminants. Ten to twenty micrograms of RNA in a volume of 5 µL was added

to 2 µL of 10X buffer, 1 µL DNase, and 12 µL RNase free water. These components were incubated for 30 minutes at 37˚C. To deactivate the DNase, 5 µL of DNase inhibiting buffer was added for 2 minutes at room temperature, and then the suspension was centrifuged for 1 minute at 13,000 rpm. The supernatant containing the cleaned RNA was transferred to a fresh tube for quantification on the NanoDrop.

The reverse transcriptase reaction was conducted with a High Capacity cDNA Reverse Transcription Kit (Applied Biosystems). An RNA sample of 4 µg in a volume of 10 µL was added to 10 µL of 2X master mix (Table 6) and mixed gently. The tubes were centrifuged briefly to eliminate air bubbles. The reaction was carried out in three steps: (i) incubation at 25˚C for 10 minutes, (ii) incubation at 37˚C for 120 minutes, and (iii) incubation at 85˚C for 5 seconds to deactivate the enzyme. This reaction yielded the cDNA sample that would be used for PCR.

Table 6 Recipe for 2X master mix for the RT reaction (Applied Biosystems).

2X Master Mix	
Component	**Volume per Reaction (µL)**
10X RT Buffer	2.0
25X dNTP Mix (100 mM)	0.8
10X RT Random Primers	2.0
Multiscribe Reverse Transcriptase	1.0
Nuclease-Free H_2O	4.2
Total Per Reaction	**10.0**

PCR was performed on the cDNA generated by the RT reaction to visualize the amount of mRNA produced by the three genes encoding NRPSs for the production of siderophores at each time point with and without Fe. PCR was performed with a thermocycler in a 25 µL reaction (Table 7). A control reaction with actin primers was included to show consistency of DNA loading. The reaction conditions in the thermocycler were as follows: 95˚C priming for 2 min, 25 cycles of (i) 95˚C strand separation for 15 seconds, (ii) 55˚C annealing for 20 seconds, and (iii) 72˚C elongation for 30 seconds, a holding period of 10 minutes at 72˚C, and a final hold at 4˚C. The PCR products were visualized on a 1.5% agarose gel with 7 µL of sample and 2 µL of 6X loading dye per lane.

Table 7 PCR reaction recipes used for amplification of cDNA produced by the reverse transcription reaction.

Component	Experimental Reactions (µL)	Actin (control) Reaction (µL)
10X Buffer (ThermoPol)	3.0	3.0
2.5 mM dNTP mix	2.5	2.5
Tap DNA Polymerase	0.25	0.25
Distilled H_2O	16.25	17.75
Primers (forward and reverse)	1.0 (10 nM)	0.25 (2.5 nM)
cDNA sample	1.0	1.0
Total Per Reaction	**25.0**	**25.0**

The experimental reactions were performed in three sets, one for each NRPS gene, and the actin control reaction.

Three primer pairs were used for each sample; one for each of the NRPS-encoding genes (*Tex21*, *Tex10*, and *Tex20*). These primers each amplified a central portion of the corresponding gene (Table 8).

Table 8 Primer sequence sets used in RT-PCR analysis of the three NRPS-encoding genes.

Primer	Sequence (5' – 3')	T_m (˚C)
*Tex20*forwardRT	GAACCTTGATAAAAACACGAAGAGC	54.7
*Tex20*reverseRT	GGCATCATCTGTCTCACAAACG	56.2
*Tex21*forwardRT	CAAAGATATCGCCACGGCTG	56.4
*Tex21*reverseRT	GGTCGCGATGATGTTTGATTG	54.6
*Tex10*ForwardRT	CAAGACGCGTTTCACCTTCTTG	56.7
*Tex10*ReverseRT	CGCTGTCCATTTGATCTCGC	56.5

The amplified region between the three primer sets is a central portion of the gene which is deleted in the mutant strains. RT stands for reverse transcriptase experiment.

In addition, RT-PCR was conducted in the same manner as above with several mutant strain samples: ΔTEX20-4, ΔTEX20-46, ΔTEX20-75, and ΔTEX10-19. These samples were grown for three days with and without Fe in the same manner as the wild type samples. For the *Tex20* mutants, *Tex20* primers were used, while *Tex10* primers were used for the ΔTEX10-19 mutant.

High Performance Liquid Chromatography Analysis of Siderophore Production

To directly analyze the amount of siderophores being secreted into the medium by the wild type and mutant *T. virens* strains, HPLC was conducted on culture filtrates or supernatants harvested at the various time points of experiment. At the time points of 3, 5, 7, and 9 days, the mycelia were harvested and used for RNA extraction, while the liquid filtrate was frozen at -80˚C until prepared for HPLC analysis. Sample preparation and HPLC analysis were conducted according to the method of (Oide *et al.*, 2006). HPLC was conducted in collaboration with the USDA Southern Plains Area Research Center, Cotton Pathology Research Unit (Dr. R. Stipanovic and Dr. L. Puckhaber). First, 100 mL of the frozen sample was thawed and $FeCl_3 \cdot 7H_2O$ was added to a concentration of 1.5 mM. This turned the liquid a light yellow color. Next, a XAD-16 column was prepared to clean the sample. The glass column used was 1 inch by 18

inches and was equipped with a stop-cock at the bottom opening. The column consisted of, from bottom to top, a thin layer of sand, 10 mL of XAD-16 (Amberlite) resin, and a top thicker layer of sand (Fig. 5). The sand was used to ensure that the resin was not washed out of the column.

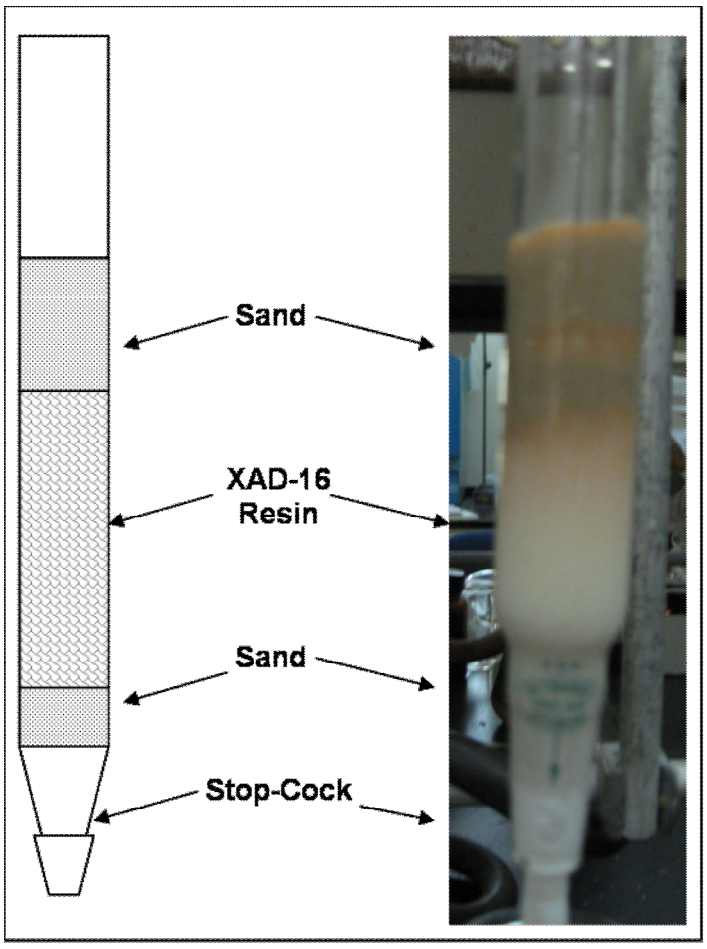

Fig. 5 Purification column. This apparatus was used to generate the crude siderophore fraction.

The column was pre-equilibrated with one column volume (10 mL) of KPO_4 buffer, pH = 7.5. Next, the culture filtrate was passed through the column and most of the yellow coloration was retained on the column. The column was then washed with 4 column volumes of KPO_4 buffer to clean the sample. The crude siderophore fraction was eluted with 3 column volumes of methanol. The first and last ten milliliters eluted were colorless and thus discarded. However, the intermediate fraction was dark orange-red and was kept for further purification. This putative siderophore fraction was dried in a roto-evaporator and then dissolved in a minimum of water (about 1 mL). If this sample would not dry, one volume of 100% ethanol was added to the sample and then dried. This sample was loaded onto four RPC18 solid phase extraction cartridges (300 mg, Alltech). Argon (Ar) gas was used to dry the loaded cartridges. Next, the siderophores were eluted from the cartridges with 3-4 mL of methanol using a syringe to force the methanol through. A dark red-orange sample was obtained. This sample was dried on the roto-evaporator to yield a solid dark orange material which was then resuspended in 500 µL of a 9:1 mixture of 15 mM acetate buffer (pH = 4.7) : acetonitrile. This sample was sealed in a glass vial and clamped with a rubber cap to be used for HPLC analysis.

A Prodigy 5 µm ODS3, 100Å column with dimensions 250 mm by 4.60 mm (Phenomenex) with a flow rate of 1 mL/min was used for HPLC. The mobile phase was A (acetonitrile) and B (15 mM acetate buffer, pH = 4.2) with a gradient elution scheme as follows: 10% A for 2 minutes, linear ramp to 60% A in 8 minutes, 60% A for 2 minutes, and linear ramp down to 10% A in 1 minute. Initially 20 µL of putative siderophore sample was loaded onto the column; however, this caused detector saturation. An injection volume of 2.0 µL was ideal. A Chem-Station Operating and Data Analysis computer program was used to analyze the chromatograms and spectra produced by the Agilent Technologies 1200 LC with diode array detector HPLC apparatus. Spectra were taken at 235 nm and 435 nm, since a broad absorption around 435 nm is characteristic of ferrated siderophores (Yu *et al.*, 2004). Twenty µL of a 40 µg/mL standard triacetylfusarinine C (TAFC) siderophore sample was run to test if this was present in the culture filtrates. The samples tested were from cultures of wild type *T. virens* at three days with and without Fe, and at five days without Fe as well as ΔTEX20-75 at three days without Fe. These choices were based on RNA expression generated by RT-PCR.

Phenotypic Characterization

Several assays were conducted on the wild type, *Tex20*, and *Tex10* (ΔTEX10-19) mutants determine the role of siderophores in basic life processes of *T. virens*. To analyze hyphal growth patterns on solid medium, a 3 mm plug was taken from the growth edge of a 1 day-old PDA plate of the different strains and placed in the center of Grimm-Allen agar plates with and without Fe in the recipe. Growth was circled after each day and these circled plates were scanned into computer files to be measured with ImageJ software.

Spore germination was assayed by spreading 1 mL of Grimm-Allen agar (± Fe) on one surface of autoclaved microscope slides. A 10 µL drop of approximately 1,000 conidia was spread onto this agar. The slides were incubated for 12 hours, viewed under 200X magnification, and the proportion of germinated spores out of the first 100 conidia observed was determined.

The conidiation assay was performed by spreading $1x10^6$ spores over a fresh PDA plate. After growth for 12 days, a 3 mm plug was taken from the plate and vortexed for 20 seconds in 1 mL of 1% triton. The concentration of the spore suspension was counted on a hemacytometer.

To test for macroscopic effects on mycoparasitism, a confrontation assay was performed between the *T. virens* strains and *Rhizoctonia solani*, a fungal plant pathogen. A 3 mm plug of each *T. virens* strain was taken from the leading edge of a colony on a 1 day-old PDA plate and placed on the perimeter of a Grimm-Allen agar plate. On the opposite edge of the plate, a plug of *R. solani* of equal size was placed. Growth and fungal interactions were observed for the next five days.

To elucidate the effect of these NRPS-encoding genes on oxidative stress response, the different strains were grown in the presence of hydrogen peroxide (H_2O_2) in conditions with and without Fe. After the Grimm-Allen medium was autoclaved and cooled to 50˚C, sufficient H_2O_2 was added to result in a concentration of 7.0 mM. These plates were inoculated with a 3 mm plug of *T. virens* taken from the growth edge of a colony from 3 day-old plate. Hyphal growth was circled for the first 4 days of incubation and growth area was measured using ImageJ software.

IV RESULTS AND DISCUSSION

Gene Module Analysis

BLASTP analysis of the NRPS-encoding genes revealed three putative NRPS-encoding genes that likely produce siderophores in the *T. virens* genome, named *Tex10*, *Tex20*, and *Tex21*. These genes were also analyzed by BLASTP for homology with other fungi. *Tex10* (4,871 amino acids) showed highest homology with NRPS2 which encodes a NRPS for ferricrocin biosynthesis in *F. graminearum* (Schwecke *et al*., 2006, Oide *et al*., 2006), *Tex20* (1,890 amino acids) shows high homology to the gene SidD which produces a NRPS for triacetylfusarinine C (TAFC) biosynthesis in *A. fumigatus* (Schrettl *et al*., 2007), and *Tex21* (1,762 amino acids) shows homology to NRPS6 which produces a NRPS for coprogen biosynthesis in *C. heterostrophus* (Oide *et al*., 2006). While TAFC and coprogen are secreted from cells (extracellular siderophores), ferricrocin is an intracellular siderophore. Each gene encoding a NRPS for putative siderophore production exhibits a unique arrangement of the condensation, thiolation, and adenylation domains (Fig. 6). These domains act in unison, as described in the literature review, to produce a unique polypeptide which will be subsequently modified to form the final siderophore product.

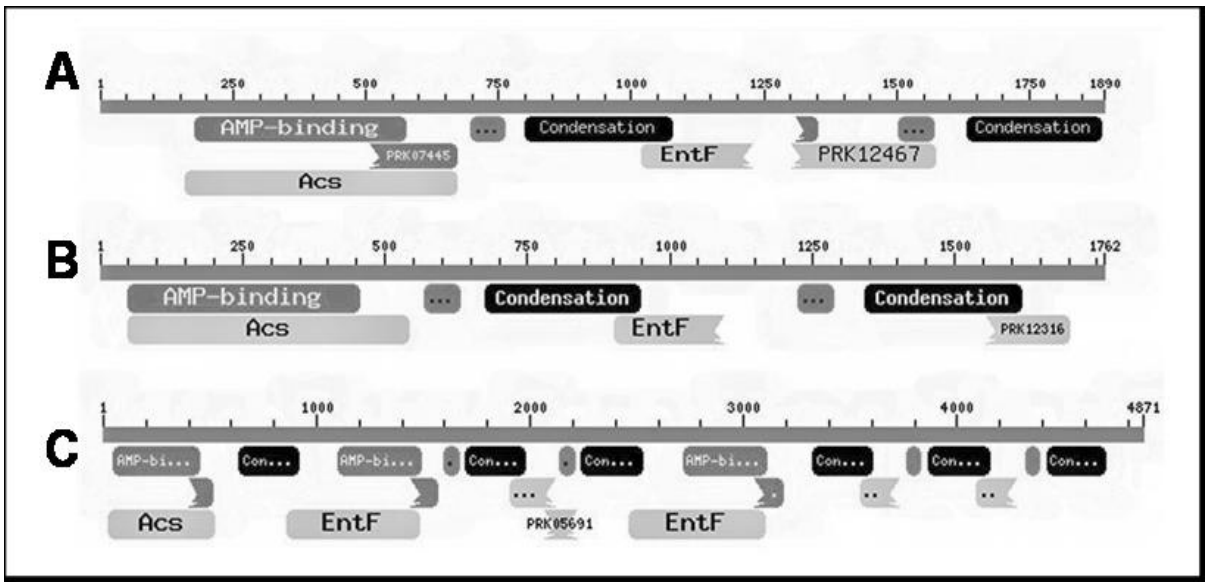

Fig. 6 Modules of the three NRPS-encoding genes that probably synthesize siderophores in *T. virens*. (A) *Tex20*, (B) *Tex 21*, (C) *Tex10*. Modular analysis was conducted using BLASTP. The (…) symbols represent thiolation domains.

Tex 21 Gene Knockout

To analyze the function of the putative NRPS-encoding genes in *T. virens*, mutants which are disrupted in the target gene were created for comparison to the wild type. A deletion cassette for *Tex21* was generated using double joint PCR which consists of three main steps (Yu *et al.*, 2004). First, the left and right flanks, representing regions of *Tex21*, as well as the central (hygromycin resistance marker) flank were amplified separately using the PCR outlined in the experimental procedure section. The PCR products were displayed on an agarose gel to validate their quality and presence (Fig. 7).

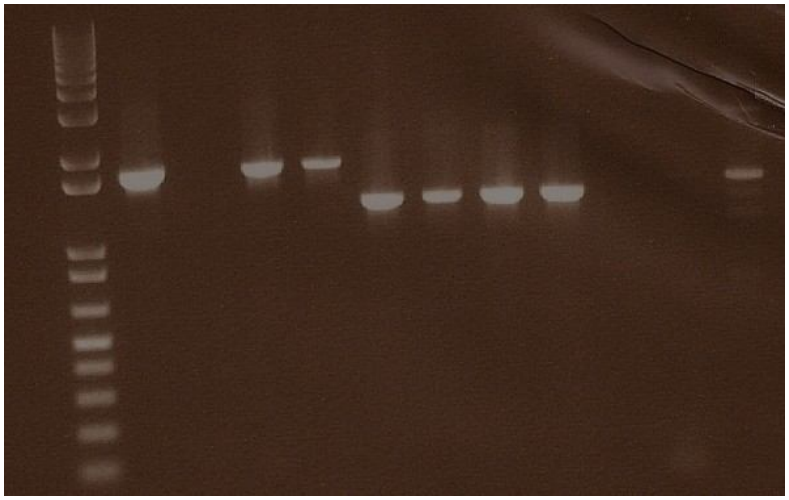

Fig. 7 Amplified flanks that will be incorporated into the construct. The first four lanes are the left flank (1.4kb), the next four are the right flank (about 1.3kb), and the last lane is the central Hyg fragment. These fragments were subsequently purified by sodium acetate precipitation before being fused in the DJ-PCR reaction.

The products of the three separate reactions (samples showing a band in Fig. 7) were combined and used in the DJ-PCR reaction after purification. Purification was necessary to remove any remaining primers in the PCR product. Quantification of each product was determined on the NanoDrop. The DJ reaction served to fuse the three flanks together due to homology between the "tails" of the left and right flank primers that overlap with the sequence of the central Hyg flank. A relatively long stretch of homology was necessary between the primer "tails" and the Hyg region so that the right

and left flank would not fuse without the Hyg in the middle. A *Tex21* deletion construct was successfully generated and was about 4.2kb in length (Fig. 8).

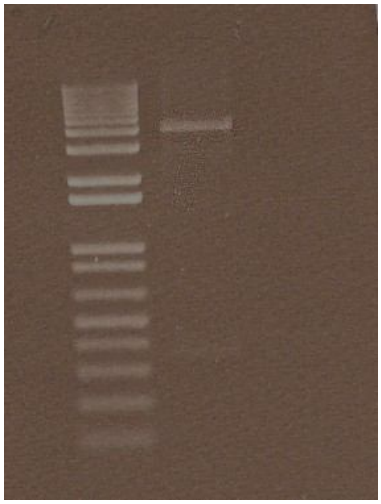

Fig. 8 *Tex 21* gene disruption cassette. A DNA agarose gel shows the complete and purified gene disruption cassette for *Tex21*. The left lane is a molecular weight marker and the right lane is the purified construct. The band is at about 4.2 kb which corresponds to the sum of the three separate fragments.

The left and right flanks of the gene disruption cassette annealed to the corresponding homologous region in the *T. virens* genome. A double crossover event between the cassette and the genome would result in the cassette replacing a central portion of the *Tex21* gene with insertion of the hygromycin resistance marker. Thus, the *Tex21* gene would be rendered incapable of encoding the NPRS, but would be resistant

to hygromycin. The cells in which this process correctly occurred would survive when grown in medium amended with hygromycin, while normal cells would die because no hygromycin resistance marker is present in the wild type genome. A deletion cassette for the ferricrocin-producing *Tex10* NRPS was also generated (Dr. Prasun Mukherjee, unpublished data) as well as for the TAFC-producing *Tex20* NRPS (Darlene Grzegorski, unpublished data). These mutant strains will allow for analysis of the function of siderophores in *T. virens.*

Tex 21 Transformation and Verification of Knockout

After transformation of the *Tex21* deletion cassette into *T. virens* protoplasts, four colonies grew through the hygromycin overlay after 1 week. These colonies were transferred to fresh Hyg medium. However they did not show noticeable growth nor did they sporulate even after several repetitions of the transformation procedure and attempts to re-isolate colonies from a Hyg plate. This is likely due to the fact that the Hyg resistance marker did not include a terminator region which may be necessary for the successful transcription of the hygromycin resistance gene that was inserted into the genome. In this case, colonies would not survive in Hyg-amended medium. A

redesigned *Tex21* deletion cassette that contains the Hyg marker containing a terminator region should be used to generate *Tex21* knockout strains.

Tex10 Verification of Knockout

Several of the *Tex10* transformants grew well in Hyg medium and sporulated at levels similar to the wild type. This indicated that the Hyg resistance marker had successfully been incorporated into the genome. Further verification of these mutants was attempted by amplifying a region that would only be present in a mutant that had the cassette inserted. The primers used for the PCR reaction would amplify a region that overlapped both the hygromycin resistance marker the region upstream of the left flank in the unmodified genome. The amplified product would be unique to a mutant and not present in the wild type. The first amplification was to determine if the left flank had integrated into the appropriate site for the targeted gene (left half of Fig. 9). A second reaction was performed to determine if the internal portion of the ferricrocin gene had been removed (right half of Fig. 9). The results of these two reactions indicated that homologous recombination had successfully occurred, but some wild type cells still existed in the culture which led to the appearance of the band that represents

amplification of the deleted region. Therefore, further purification of this culture was necessary.

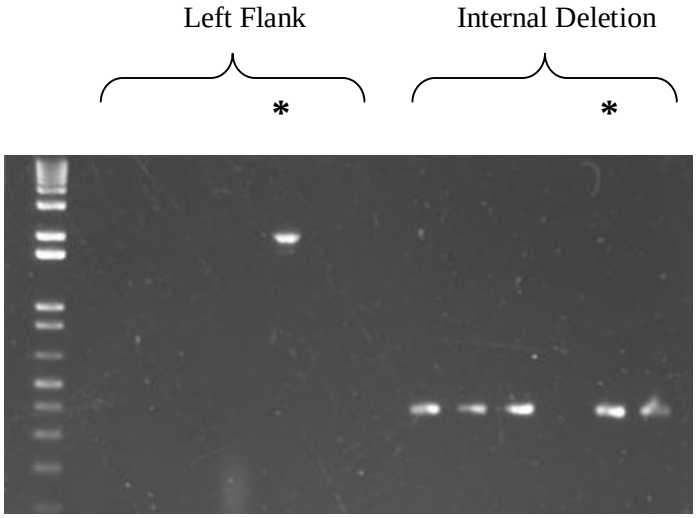

Fig. 9 DNA agarose gel of PCR screening of *Tex10* transformants. The homologous recombination test reactions (left flank) used the two Hph primers (from the Hyg segment) and the internal deletion test reactions used the *Tex10* forward and reverse primers listed in Table 4 (above). Five transformants were tested along with the wild type (the last lane in each set). The transformant of interest, number 19, is indicated with an asterisk.

Tex20 Verification of Knockout

Previous to my study, the Kenerley laboratory had transformed an auxotrophic strain of *T. virens* (Tv10.4, see Experimental Procedures) to disrupt *Tex20*. To verify this mutation, southern blotting was performed (Darlene Grzegorski, unpublished data).

Southern blotting is a technique by which a radio-labeled DNA probe is hybridized to homologous regions of the fragmented genome which has been digested by a specific restriction enzyme, thus revealing the presence or absence of a segment of DNA. This technique revealed the effective knockout of *Tex20* in several transformants (Fig. 10). From these, Δ*Tex20 #* 4, 46, and 75 were chosen for further analysis.

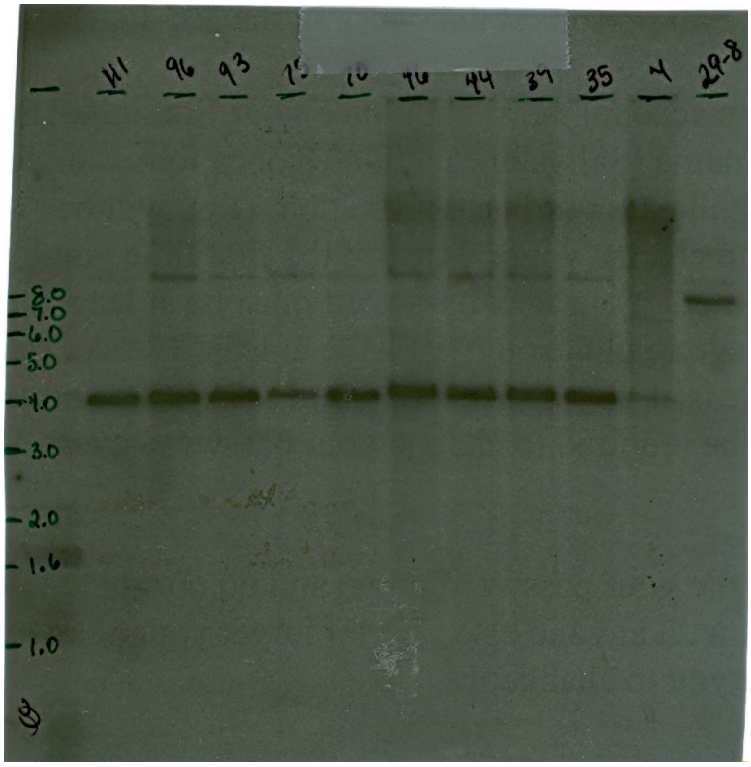

Fig. 10 Southern blot of *Tex20* transformants. This verifies *Tex20* gene deletion (Darlene Grzegorski, unpublished data). A band at 8kb is expected in the wild type (29-8) and a band at 4 kb is expected in the knock outs (numbered). The knockouts utilized in the remaining experiments were numbers 4, 46 and 75. The probe was a 1.3 kb fragment from an Apa/Kpn digest of the PDXG75 vector.

Generation of mutant strains is vital for the analysis of siderophore activity, since the production patterns and functions of the mutant strains can be compared with those of the wild type. Several mutant strains are now available for further analysis of siderophore activity. These are ΔTEX10-19, a *Tex10* mutant, and three *Tex20* mutants: ΔTEX20-4, ΔTEX20-46, and ΔTEX20-75.

Wild Type Gene Expression Profile

An expression profile of the genes that encode the NRPSs that synthesize siderophores in the wild type is required to understand siderophore production and activity. For this reason, the mRNA production pattern of each of the three genes, *Tex10*, *Tex20*, and *Tex21*, was experimentally determined using reverse-transcriptase PCR (RT-PCR). This is a technique that reflects gene expression levels by converting mRNA extracted from cells into DNA that can be analyzed by PCR with primers to suit the experimental purpose.

In other microbes, siderophores are known to be produced under conditions of Fe deprivation, while their production decreases or ceases in high-Fe conditions. Thus, the presence of absence of Fe was one parameter under which expression of genes encoding NRPSs was tested. Wild type was grown in Grimm-Allen medium with or without Fe.

The second parameter was incubation period; 1, 3, 5, 7, and 9 days. This experimental design would answer two questions: (i) how do the expression levels of the three genes produced under Fe deprivation compare with those under high-Fe conditions? and (ii) what is the temporal gene expression pattern?

The Grimm-Allen medium used is a very minimal medium therefore, after 1 day of growth no measurable amount of mycelia was present in the liquid cultures. However, mycelia were harvested for the periods from 3 – 9 days. To assess the integrity of the RNA extraction, a 1% agarose gel was run and stained with ethidium bromide. The presence of two close bands indicates 28S and 18S ribosomal RNA (rRNA) and thus an intact mRNA sample (Fig. 11).

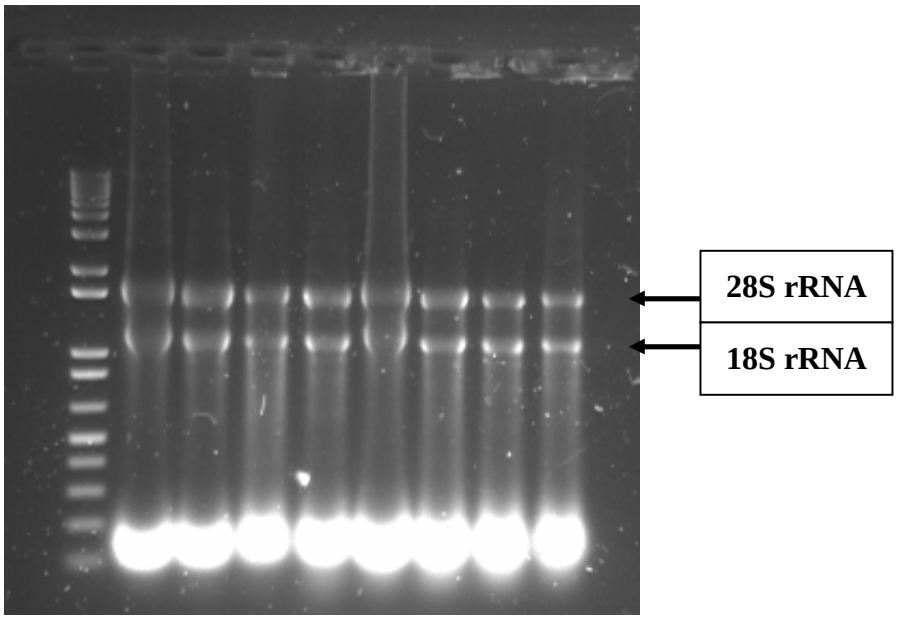

Fig. 11 Initial RNA samples. A 1% agarose gel of extracted RNA samples (after DNase cleaning) indicates two bands for rRNA and some degradation at the bottom of the gel. From left to right, the wells are: 1kb plus marker, 3 days growth +Fe, 3 days growth –Fe, 5 days ±Fe, 7 days ±Fe, 9 days ±Fe.

As a control for the amount of cDNA loaded into each well for the PCR reaction of the cDNA generated by the RT reaction, actin primers were used applied to each cDNA sample. In addition, a negative control was conducted to eliminate the possibility that the PCR reaction was contaminated with extraneous DNA. This control reaction consisted of all the PCR ingredients listed in the experimental procedures section except for the sample cDNA.

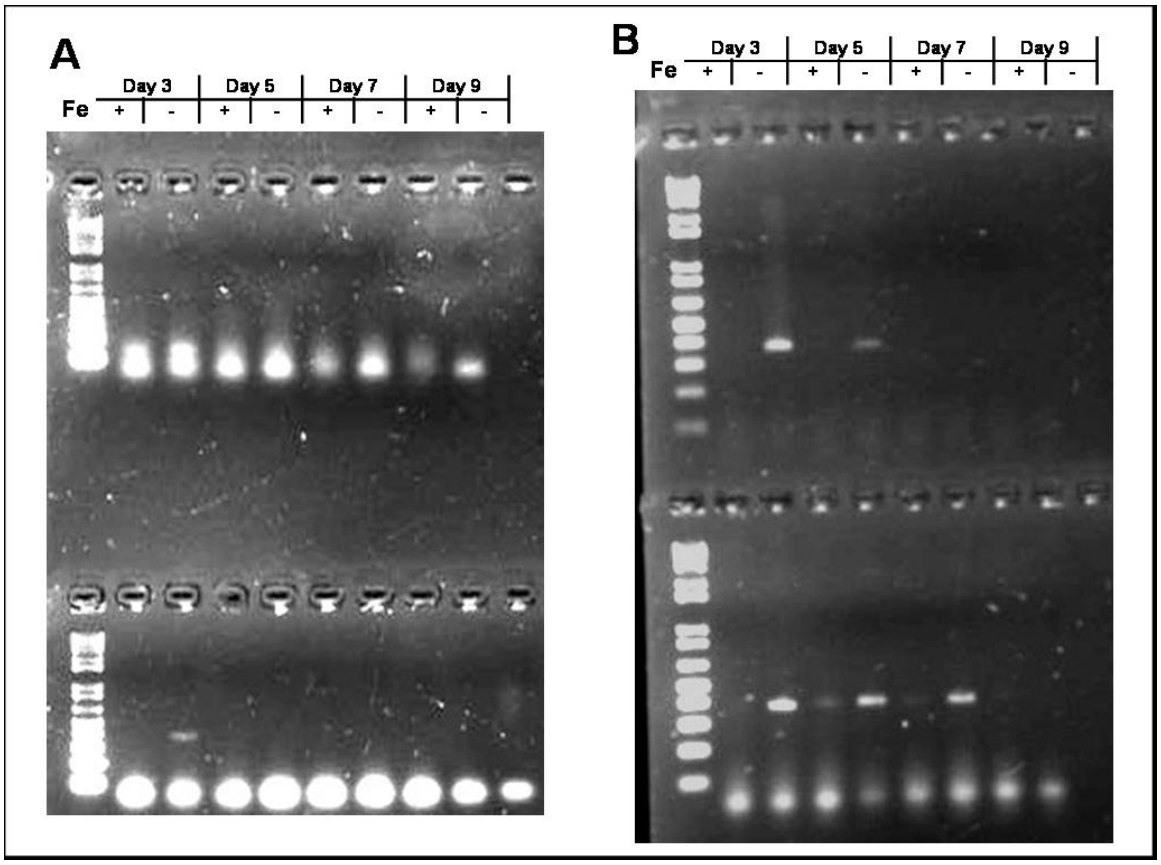

Fig. 12 RT-PCR results**.** 1.5% agarose gels of products of the PCR reaction were run on the cDNA generated by the RT reaction of the eight mycelial samples. The last lane on each gel is the negative control. The primer sets used were: (A) top– actin, bottom- *Tex20*, and (B) top- *Tex21*, bottom- *Tex10*.

The lanes with the negative control reactions are all empty (except for the primer-dimer in the *Tex20* sample) which validates the PCR reaction. The actin reaction reveals that the amount of cDNA loaded into each lane is sufficiently consistent for comparison between samples. These gels (Fig. 12) reveal the expression profile of the three NRPS-encoding genes, *Tex10*, *Tex20*, and *Tex21*. A band on the gel indicates

amplification (via PCR) of a region of the corresponding gene in the cDNA, which indicates mRNA for this gene was present in the cell at the time RNA was extracted. The strong band at three days without Fe for all three genes indicates that these genes are "turned on" and producing mRNA under Fe deprivation. All three genes show highest induction at three days under Fe deprivation. *Tex21* also shows distinctive expression at 5 days without Fe. Even more interesting, *Tex10*, the gene that encodes the siderophore ferricrocin, shows high expression at 5 and 7 days without Fe. Gene expression was absent when Fe was abundant in the medium at any time point tested. Also, no bands are seen at nine days in any of the reactions. This could be due to silencing of the gene at this point in the organism's life cycle, mRNA degradation by the fungus, or because the fungus reached stationary phase and was not actively producing these enzymes. These band patterns indicate that siderophores expression in *T. virens* is similar as in other microbes: siderophores are expressed when Fe is scarce in the environment. This shows that in low Fe conditions, siderophore secretion could be a vital mechanism for *T. virens* to scavenge the very low concentrations of Fe that exist in the medium. Up-regulation of *Tex10* suggests the need for enhanced Fe storage capabilities under low- Fe conditions since its homologue encodes an NRPS for ferricrocin biosynthesis, an intracellular

siderophore, in *C. heterostrophus* (Oide *et al.*, 2006). This could be due to, in part, to the increased uptake of Fe the cells are experiencing due to up-regulation of the genes that produce extracellular siderophores via NRPSs (coprogen and TAFC). This expression profile is a vital basis for further siderophore studies in *T. virens* and was also necessary to choose which conditions to test in the HPLC experiment for siderophore production.

Mutant gene expression

In order to verify that mRNA production of the corresponding NRPS-encoding gene had been abolished in the mutant strains, RT-PCR was conducted on mycelial samples that were grown, collected, and treated in the same manner as the wild type. Amplification of actin was, again, used as a control for the amount of DNA loaded into each lane. Each mutant was analyzed at three days of growth with and without Fe as this was the time in which e the wild type sample showed highest mRNA levels for all three genes. Thus, the cDNA generated from the ΔTEX10-19 sample was tested with primers to amplify an internal region of the *Tex10* gene (Table 8). The cDNA generated from the ΔTEX20-4, ΔTEX20-46, and ΔTEX20-75 samples was tested with primers to amplify an internal region of the *Tex20* gene (Table 8). The PCR products are displayed on 1.5% agarose gels stained with ethidium bromide (Fig. 13). The presence of a strong band in

the *Tex10* reaction for wild type without Fe is to be expected (as shown in Fig. 12). There is also a visible band in the ΔTEX10-19 sample without Fe, thus indicating the presence of wild type cell contaminants in the mutant sample. However, this band is distinctively lighter than the wild type band, thus indicating that *Tex10* mRNA levels are lower in this mutant than in the wild type. The *Tex20* gel reveals that only the wild type without Fe sample produces *Tex20* mRNA. None of the ΔTEX20 mutants tested show any band in this reaction, thus revealing these mutants are not producing any mRNA and are thus deficient in the *Tex20* gene.

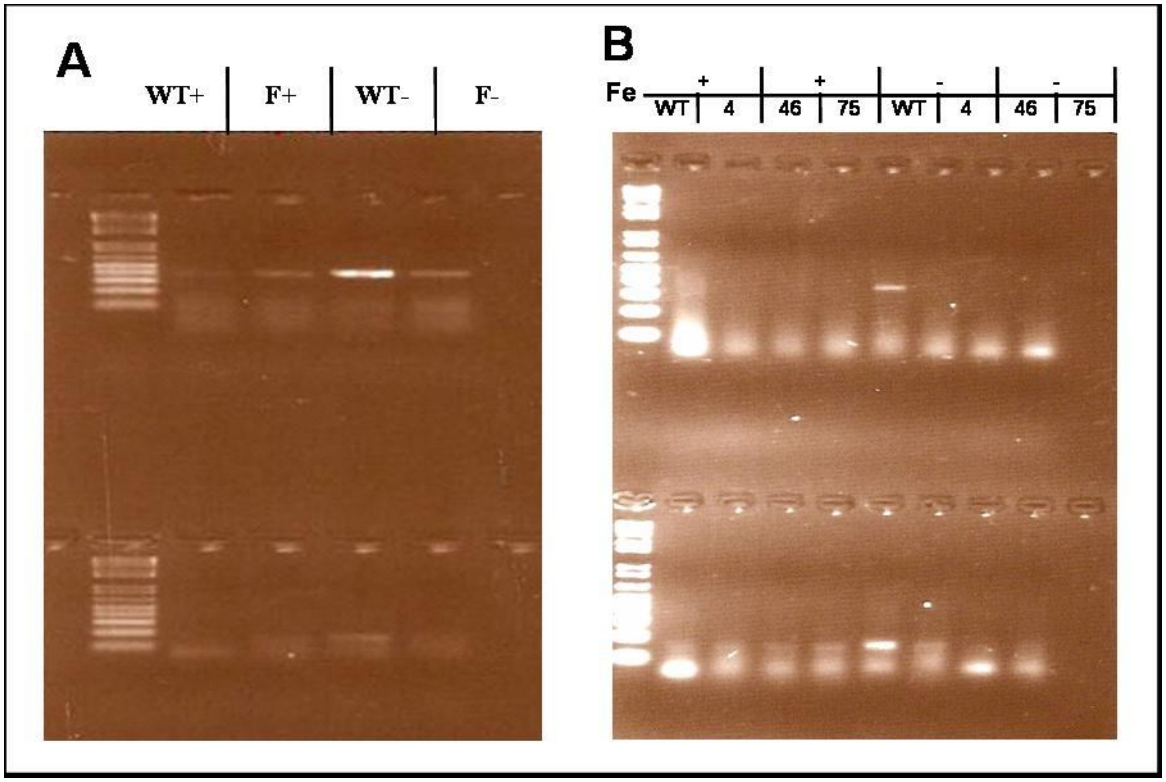

Fig. 13 Mutant RT-PCR results. 1.5% agarose gels of RT-PCR products derived from wild type and four mutant strains (ΔTEX20-4, ΔTEX20-46, ΔTEX20-75, and ΔTEX10-19) were run. A band indicates the presence of the corresponding gene. The primers used are listed in Table 8. Abbreviations: WT (wild type sample), + (grown with Fe), - (grown without Fe), F (ΔTEX10-19 sample), 4 (ΔTEX20-4), 46 (ΔTEX20-46), and 75 (ΔTEX20-75). The primer sets used were: actin for both bottom gels (A) top- *Tex10,* (B) top- *Tex20*.

Analysis of Siderophore Production

The presence of siderophores secreted into the liquid culture by *T. virens* was determined by HPLC. The column used was a reverse-phase C18 column which is nonpolar and consists of n-octyldecyl side groups linked to a siloxane backbone (Skoog,

2007). Extensive purification of the culture filtrate samples was necessary to prepare them for HPLC analysis. Elution through the XAD-16 resin was the first step to clean the sample. The sample's red/orange coloration was retained in this resin until it was eluted with methanol to give a dark red fraction. The samples were further purified by passage through an RPC18 solid phase extraction cartridge (Alltech). After these purification procedures, the sample was ready for HPLC analysis.

Spectra of each sample were obtained at 254 nm and 435 nm. Most compounds absorb at 254 nm, so this wavelength is not specific to siderophores. However, siderophores uniquely absorb at 435 nm while most other compounds do not (Konetschny-Rapp, 1988). The absorbance spectrum of a siderophore resembles a low, broad peak spanning approximately 350 nm to 550 nm. These determinants were used to ascertain the presence of siderophores based on the peaks in the chromatograms and the shape of the absorbance spectrum from 350-550 nm. As a siderophore standard, 20 µL of 40 µg/mL TAFC was found to have a retention time of 9.696 minutes with a peak area of 60.63 mAU*sec at 435nm (Fig. 14). The characteristic siderophore spectrum is exemplified by that of the TAFC standard (Fig. 15). It shows a broad absorbance from about 350 – 550 nm.

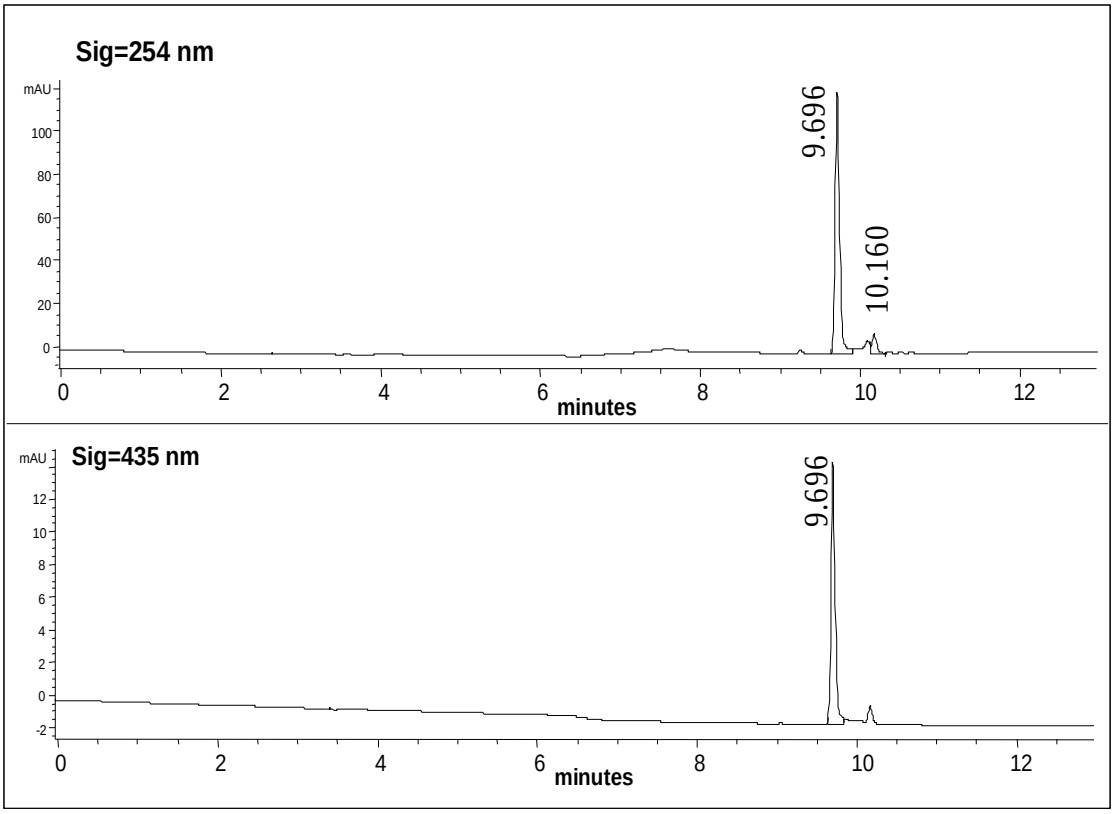

Fig. 14 Chromatograms taken for the TAFC standard (40 µg/mL). 20 µL of sample were loaded. The retention times (R_T) are written by each peak (in minutes).

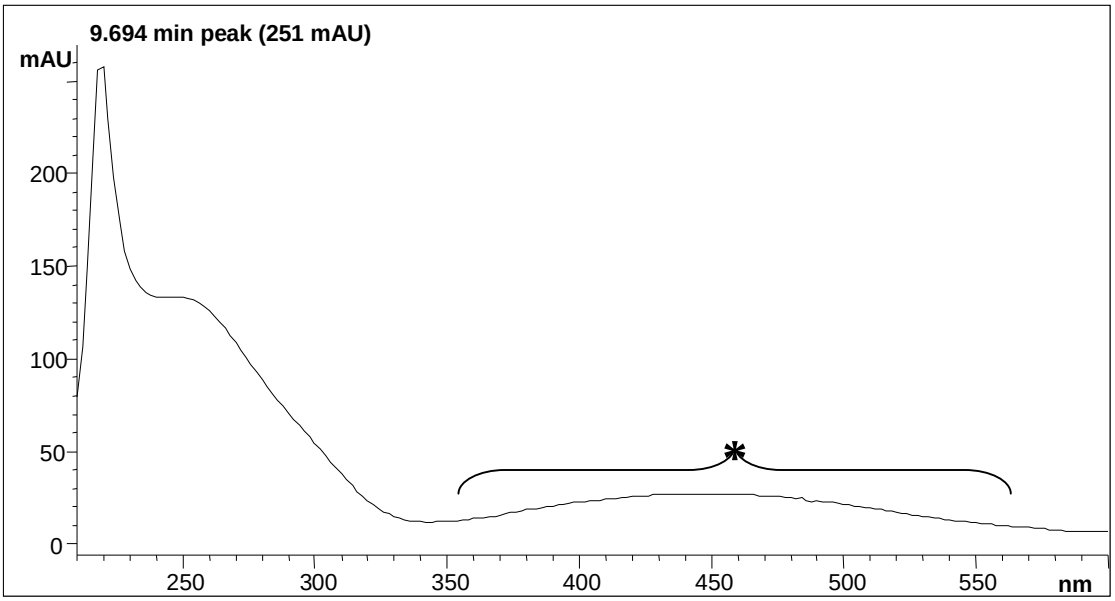

Fig. 15 TAFC standard absorbance spectrum. This is the total absorbance spectrum of the peak with R_T= 9.694 minutes. The broad absorbance (*) is characteristic of and unique to siderophores (Konetschny-Rapp, 1988).

The culture filtrates to be assayed were chosen based on gene expression profiles. Wild type samples were tested from the 3 day treatment (±Fe) and the 5 day treatment (-Fe). Also, a sample of ΔTEX20-75 culture filtrate from 3 days growing without Fe was tested to determine whether or not extracellular siderophores were being produced in this mutant. Initially, 20 µL of sample was injected into the HPLC for analysis; however this led to detector saturation as the samples were too concentrated for the diode array detector (DAD) (Fig. 16).

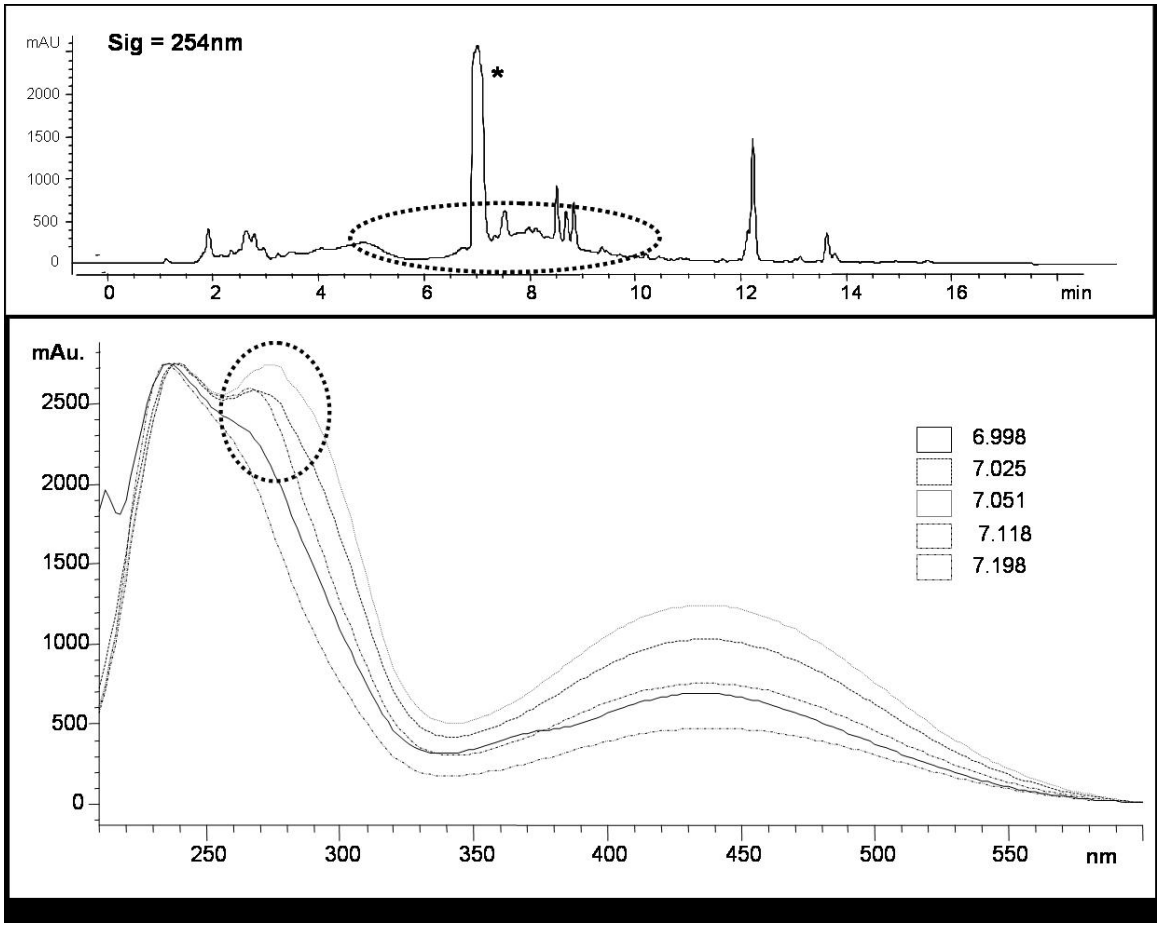

Fig. 16 Detector saturation. A Chromatogram (top) and spectrum (bottom) are showing detector saturation due to overloading the column with a concentrated sample. 20 µL was loaded of wild type grown for three days without Fe. The spectrum consists of five total absorbance spectra, each taken at a different point the peak from the chromatogram at 7.073 minutes (*). The encircled region indicates effects due to detector saturation.

To avoid detector saturation, only 2 µL was loaded onto the column for each of the remaining samples. When this volume was run for the wild type sample grown for three days under Fe deprivation, a significant amount of siderophore was observed in the

chromatogram taken at 435 nm. This large peak had a retention time of 7.078 minutes and an area of 799.76 mAU*sec. However, an obvious shoulder peak was present at 7.206 minutes and was fused with the primary peak. The total absorbance spectra of each peak indicate that they are each, indeed, siderophores (due to the broad absorbance pattern) and due to their different retention times, they are distinct from one another (Fig. 17). This indicated that two siderophores were present in the culture filtrate of this sample. However, this R_T is very distinct from that of the TAFC standard; therefore these detected siderophores are not TAFC.

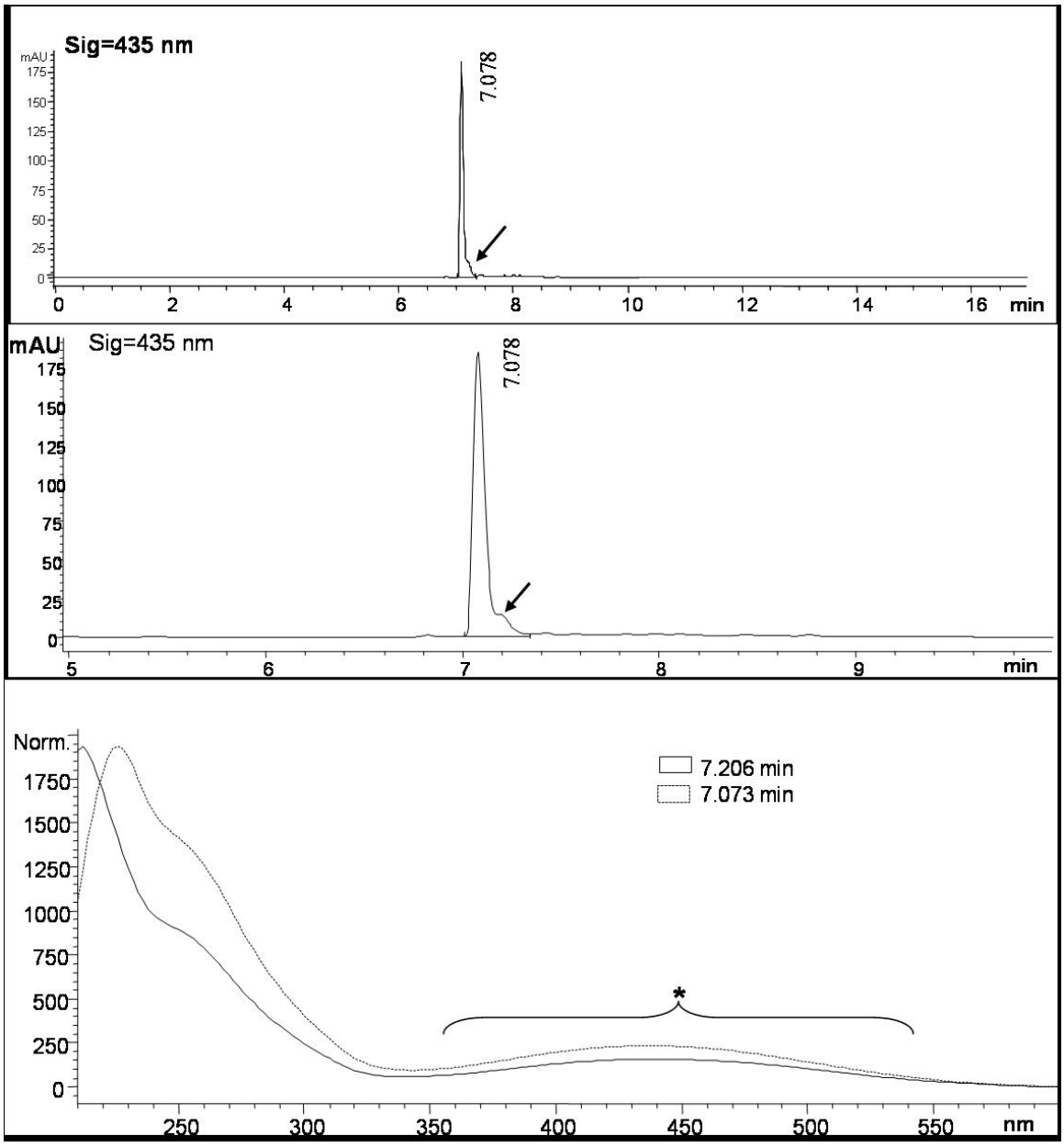

Fig. 17 HPLC results for wild type grown 3 days without Fe. Chromatograms (top two) and spectrum (bottom) of wild type sample grown for three days under Fe deprivation. The peak at 7.078 min is a siderophore as indicated by the characteristics of the absorbance spectrum (*, dotted line). The shoulder peak is indicated by the arrow and the time scale is shortened in the second chromatogram to distinguish the shoulder peak which represents a distinct siderophore from the primary peak. This shoulder peak is also a siderophore, as indicated by the absorbance spectrum (solid line).

To verify that siderophore production was decreased when *T. virens* is grown with Fe abundant in the medium, a sample of wild type grown for 3 days with Fe was analyzed by HPLC. This sample resulted in a peak at 435 nm at the same R_T as that of the sample without Fe. However, this peak is dramatically smaller compared to cultures without Fe. Culture filtrates from samples of the wild type growing without Fe yielded a peak area of about 800 mAU*sec while samples from cultures grown with Fe gave a peak area of about 5.2 mAU*sec (Fig. 18). The peak at R_T=7.053 minutes was the only one out of several peaks that is actually a siderophore. The total absorbance spectrum of each peak that was present at 425 nm was analyzed, and the only spectrum that exhibited the characteristic siderophore absorbance pattern was that with R_T = 7.053 minutes.

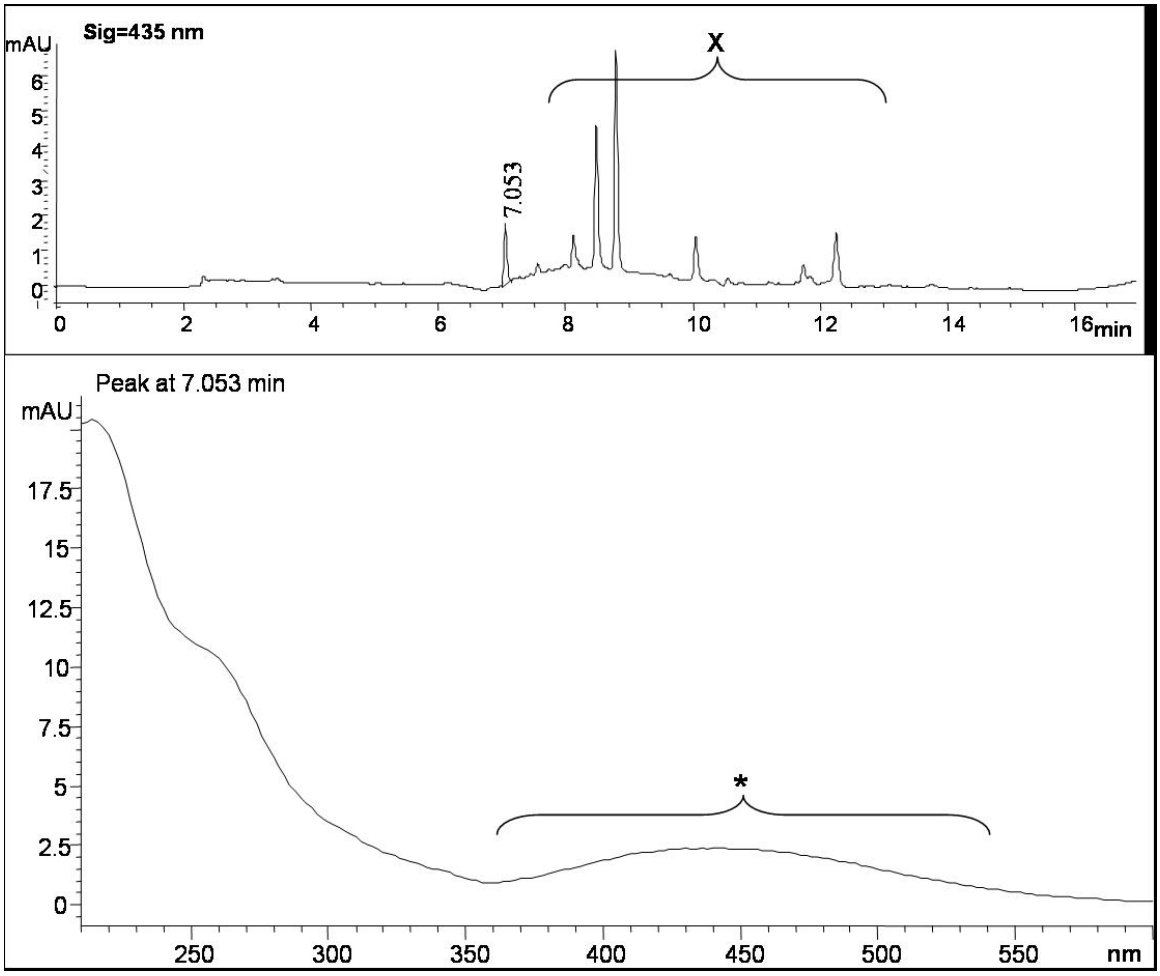

Fig. 18 HPLC results for wild type grown 3 days with Fe. Chromatogram (top) and total absorbance spectrum (bottom) of a sample of wild type grown for three days with abundant Fe. From the chromatogram (at 435 nm), a spectrum was taken for each peak. The peaks bracketed by "X" did not show the characteristic siderophore absorption, as did the peak with R_T=7.053 minutes whose absorbance spectrum is indicative of siderophores (*). The spectrum was taken at the apex of the 7.053 minute peak.

The gene expression profile generated in the RT-PCR experiment for the wild type indicated siderophores should be also present after 5 days of growth without Fe.

Therefore, this condition was tested with HPLC. One siderophore peak was present at 435 nm with R_T = 7.050 minutes. This peak had an area of about 89 mAU*sec at 1/3 the concentration of all other samples (Fig. 19). Although these HPLC analyses were not quantitative, general comparisons can be made because all fungal samples were grown with the same constants; the beginning volume before purification for HPLC was the same, and the method to prepare and conduct HPLC was identical. The only experimental difference is that the crude siderophore sample grown for 5 days without Fe was resuspended in a volume 3 times greater than the other samples before HPLC analysis. Therefore, if this sample were at the same concentration as the others, its theoretical peak area could be approximately 270 mAU*sec. This value is significantly lower than the peak area (with the same R_T) for the wild type grown for 3 days without Fe. This corresponds with gene expression for *Tex21* which shows the largest band at 3 days without Fe and a smaller one at 5 days without Fe. Furthermore, no shoulder peak is present in this sample.

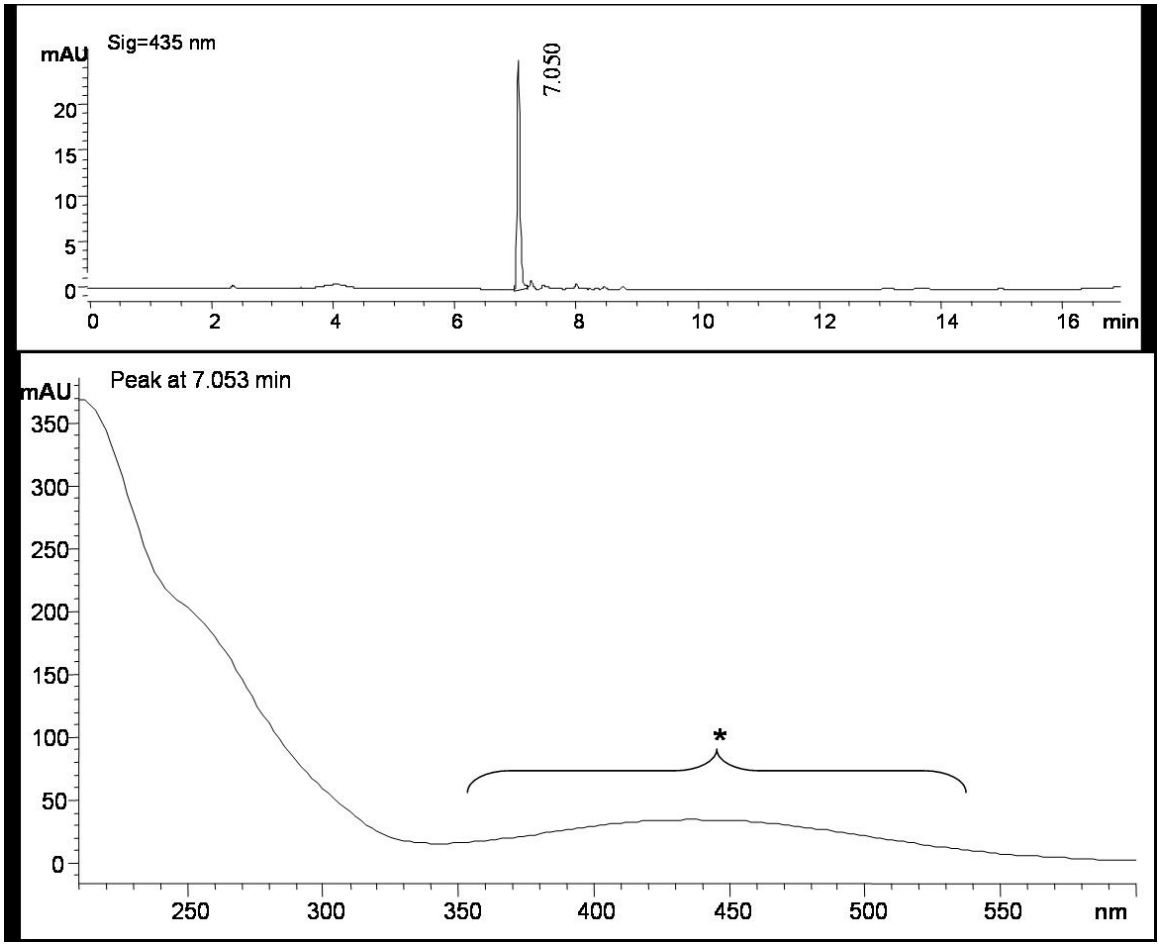

Fig. 19 HPLC results for wild type grown 5 days without Fe. Chromatogram (top) and total absorbance spectrum (bottom) of a sample of wild type grown for five days without Fe. From the main peak (in the chromatogram at 435 nm), a spectrum was taken. The peak with R_T=7.050 minutes has an absorbance spectrum that is indicative of siderophores (*). The spectrum was taken from the apex of the 7.050 minute peak.

One mutant, ΔTEX20-75, was analyzed by HPLC after growth for three days without Fe as an analysis of the correspondence of gene expression with direct measurement of siderophores. No gene expression of *Tex20* was demonstrated for this

condition. The chromatogram of this sample showed a siderophore peak at the same time as the other samples (R_T=7.030 minutes), but its area is dramatically reduced to 19.8 mAU*sec (Fig. 20). Thus, the knockout of the *Tex20* gene is causing a dramatic decrease in the production of this siderophore.

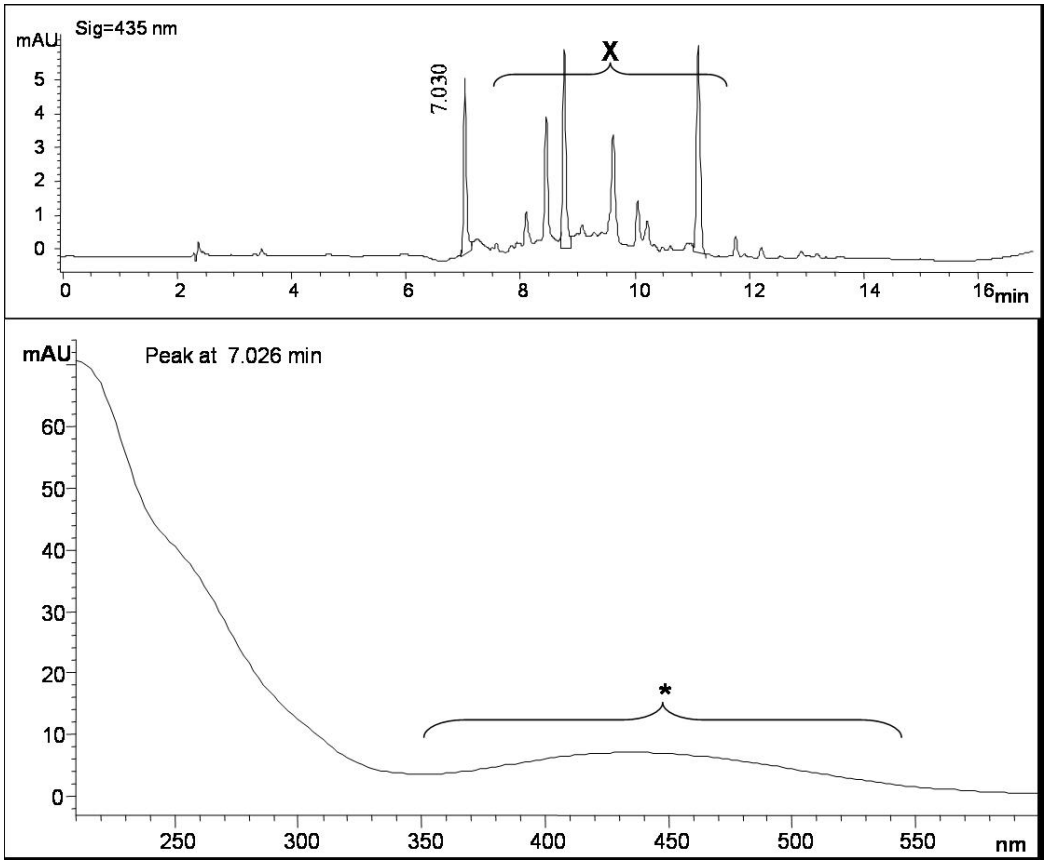

Fig. 20 HPLC results for ΔTEX20-75 grown 3 days without Fe. Chromatogram (top) and total absorbance spectrum (bottom) of a sample of ΔTEX20-75 grown for three days without Fe. From the chromatogram (at 435 nm), a spectrum was taken for each peak. The peaks bracketed by "X" did not show the characteristic siderophore absorption, as the peak did with R_T=7.030 minutes; this absorbance spectrum is indicative of siderophores (*). The spectrum was taken at the apex of the 7.030 minute peak.

Overall, the patterns of siderophore production are in accordance with gene expression. This siderophore is being produced under conditions of Fe deprivation and its production is dramatically reduced in high-Fe growth conditions. The highest production of the siderophores is at three days with a reduced amount at five days of growth. These conclusions all match the expectations generated by the RT-PCR experiments. This siderophore (and the shoulder siderophore in the wild type sample grown for 3 days without Fe) is not TAFC, since its retention time is so distinct from that of the standard TAFC. Although it is certain these peaks at 435 nm represent siderophores, the compounds cannot be identified with certainty until other siderophore standards are assayed by the same HPLC conditions or by analyzing the fraction by MS/MS (tandem mass spectrometry) and MALDI-TOF (matrix-assisted laser desorption/ionization time of flight) mass spectrometry. The results of the HPLC experiment are summarized in Table 9.

Table 9 Summary of HPLC results for all four fungal samples tested.

Sample	R_T (primary peak, min)	R_T (shoulder peak, min)	Primary Peak Area (mAU*sec)	Final V_{total} (mL)	Theoretical Peak Area (mAU*sec)
WT, 3d, -Fe	7.078	7.206	799.7577	0.5	799.7577
WT, 3d, +Fe	7.053	n/a	5.1723	0.5	5.1723
WT, 5d, -Fe	7.05	n/a	89.1042	1.5	267.3126
ΔTEX20-75, 3d, -Fe	7.03	n/a	19.8142	0.5	19.8142

The theoretical peak area was calculated by setting the baseline volume at 0.5 mL. Thus, the WT, 5d –Fe sample's peak area was multiplied by 3 to obtain a value that was comparable to the others. WT (wild type), 3d (3 days growth), 5d (5 days growth), R_T (retention time), mAU (milli-absorbance-units), V_{total} (total volume of siderophore fraction after purification process).

Phenotypic Characterization

To determine the effect of disrupting the genes that encode NRPSs that biosynthesize siderophores on the basic life processes of *T. virens*, several phenotypic assays were conducted using the wild type, *Tex10* mutant, and *Tex20* mutants. These assays may also reveal relationships between the three siderophores (2 extracellular and 1 intracellular) that are present in *T. virens*. The characteristics that were analyzed were hyphal growth, spore germination, spore production, mycoparasitism, and resistance to oxidative stress.

Fungal expansion or growth can be determined in vitro on solid medium by measuring the area of the hyphae which extend radially from the point of inoculation. The area occupied by hyphae was recorded by marking the growing edge with the area assessed by ImageJ software. All four mutant strains (ΔTEX10-19, ΔTEX20-4, ΔTEX20-46, and ΔTEX20-75) were compared with the wild type after one and two days of growth on solid medium with and without Fe (Fig. 21). The only mutant that grew significantly different from the wild type was ΔTEX10-19. This mutant grew significantly slower than the wild type on medium with or without Fe at one and two days. Even when Fe is present in the medium, this mutant is unable to grow at a normal rate. This indicates that the problem is not with Fe acquisition because it is readily available in the growth medium. If the gene *Tex10* encodes the NRPS for the synthesis of the intercellular siderophore ferricrocin, the slow growth may be attributed to the inability of this mutant to store Fe inside the cell. Contrastingly, the ΔTEX20 mutants do not show significantly reduced growth at one or two days whether or not Fe was present in the medium. If *Tex20* encodes an NRPS for extracellular biosynthesis, in the low Fe medium when siderophores are necessary to uptake any available Fe, one possibility is

that the two extracellular siderophores can compensate for each other when one is not synthesized or synthesized in very small concentrations.

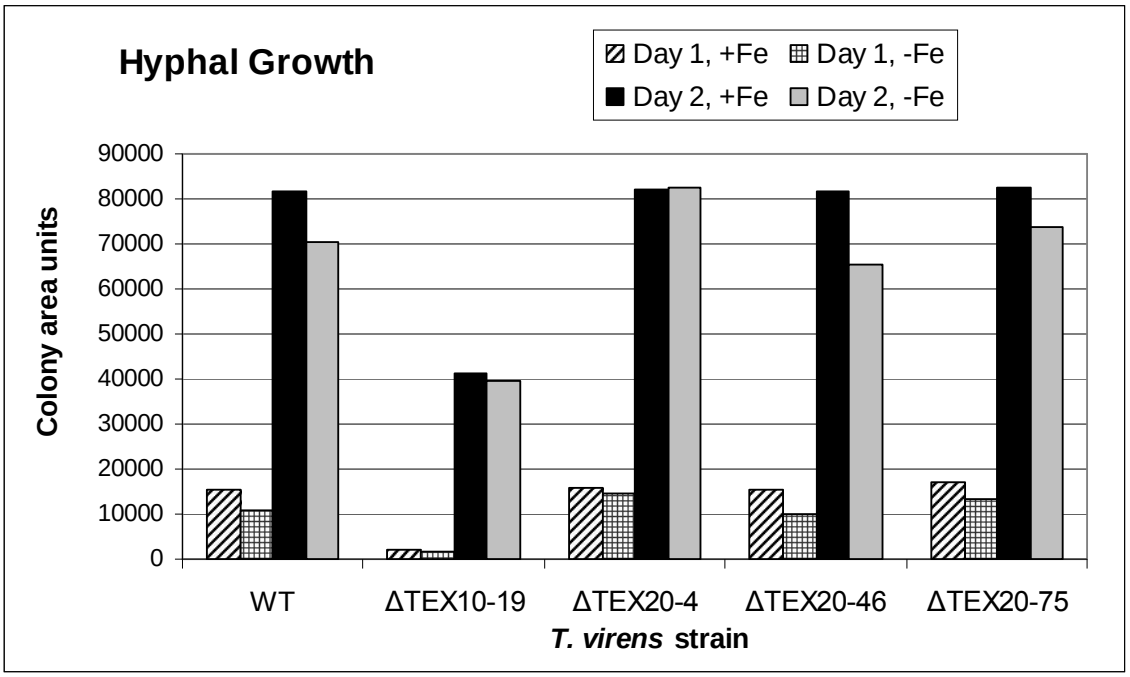

Fig. 21 Hyphal growth. Hyphal area of the mutant and wild type strains was measured at 1 and 2 days of growth on solid medium with and without Fe. Colony area units are arbitrary units from the ImageJ software.

One aspect of the life cycle of T. virens is the capacity to reproduce by the production of asexual spores or conidia. This ability was assayed for each strain (ΔTEX10-19, ΔTEX20-4, ΔTEX20-46, and ΔTEX20-75) under high and low Fe conditions. The quantity of spores produced by the ΔTEX10-19 mutant was lower than

wild type, but not significant according to analysis of variance (ANOVA, http://faculty.vassar.edu/lowry//anova1u.html). The average value of spores counted from the wild type in the assay was 142, while that of ΔTEX10-19 was 90 (Fig. 22). If indeed ΔTEX10-19 is disrupted in the ability to synthesize ferricrocin, then this may indicate that intracellular Fe storage by siderophores is clearly an integral part of the process of spore production.

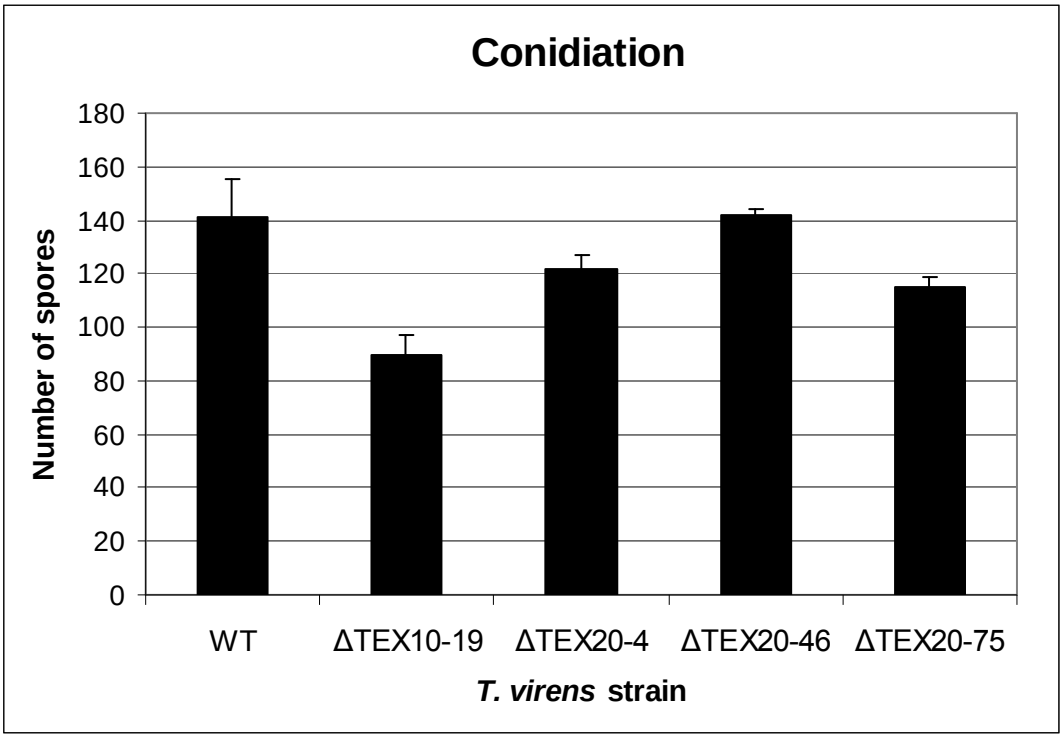

Fig. 22 Conidiation. Spore production of each mutant strain and the wild type was tested. The number of spores based on the count of spores released from a 3mm mycelial plug was counted. Data presented are the average of a duplicate experiment. Standard error bars are shown.

Another aspect of the life cycle of *T. virens* is the ability of the spores to germinate. Therefore, a spore germination assay was conducted to determine if differences existed between the ability of the wild type and mutants to produce spores that germinate normally. This was measured by counting the proportion of germinated spores out of the first 100 total spores viewed under a microscope (Fig. 23). This was tested under low and high Fe conditions. In low Fe medium, wild type showed 80.3% germination rate, while ΔTEX10-19 showed only 12.6% germination rate. If the *Tex10* gene encodes the NRPS which produces the intracellular siderophore ferricrocin, this implicates the role of cellular Fe storage by intracellular siderophores in the process of spore germination. This is affirmed because even when Fe is abundant in the medium, germination is only 30.7% in the ΔTEX10-19 mutant as opposed to 86.3% in the wild type. Thus, whether Fe is available for normal uptake or it must be imported by siderophores, if the cells cannot store the Fe using ferricrocin, they do not function normally. Furthermore, all three ΔTEX20 mutants show decreased percentages of germination compared to the wild type. This does suggest that the secretion and activity of extracellular siderophore are events involved in spore germination. The percentages in these mutants are much higher than with ΔTEX10-19 which may indicate that

extracellular siderophores may compensate each other when one is absent or greatly reduced.

The percentages in these mutants are still relatively high (compared to the ferricrocin mutant) which suggests that the other extracellular siderophore is helping to compensate for the lack of the siderophore produced by *Tex20*'s NRPS. ANOVA was carried out to compare each mutant to the wild type and the results are provided in the legend of Fig. 23. Each mutant was significantly different from the corresponding wild type treatment with the exception of ΔTEX20-4 without Fe.

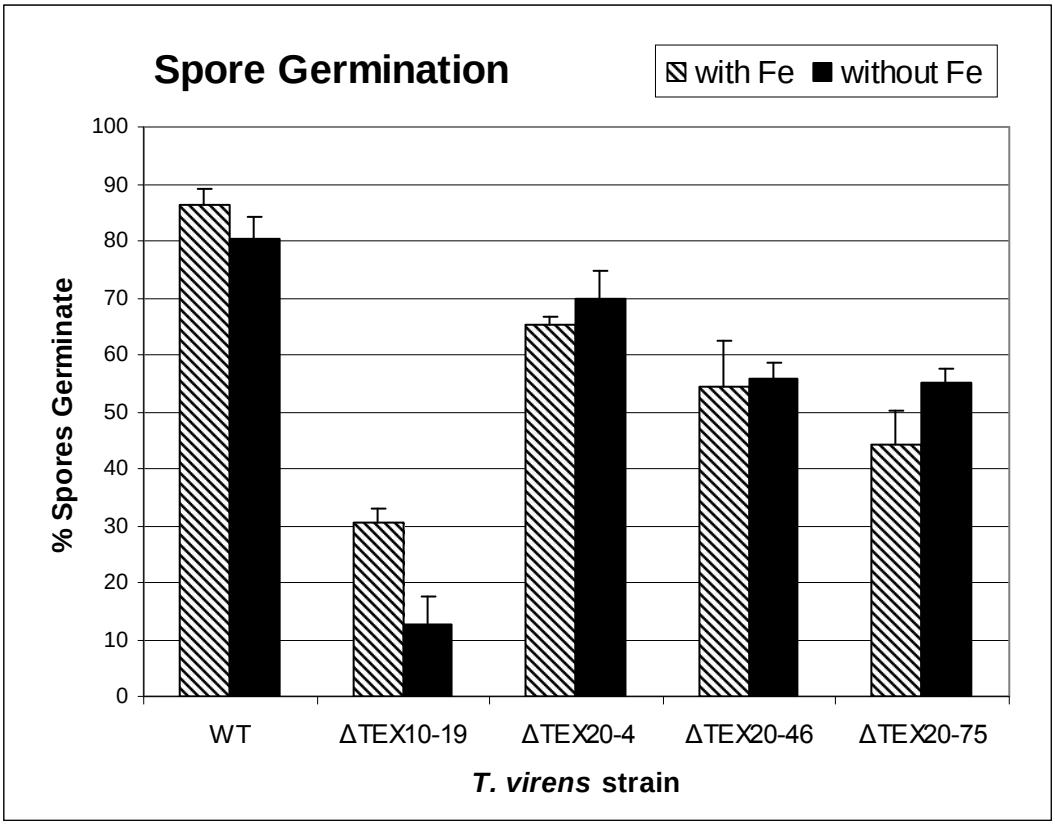

Fig. 23 Spore germination**.** The percentage of spores germinated was measured for the wild type and four mutants both with and without Fe on solid medium. Spores were inoculated onto microscope slides covered in agar and incubated for 12 hours. The number of germinated spores out of the first 100 viewed under the microscope was counted. Data presented are the average of a triplicate experiment. Standard error bars are shown for each data set. ANOVA results: ΔTEX10-19 ±Fe ($p<0.0004$); ΔTEX20-4 +Fe ($p<0.003$); ΔTEX20-46 +Fe ($p<0.03$); ΔTEX20-4 –Fe ($p<0.007$); ΔTEX20-75 ±Fe ($p<0.005$).

The effect the disruption of genes encoding the selected NRPS genes on mycoparasitism was assayed in vitro on solid medium against the plant pathogen *R. solani*. The mutants or wild type were placed opposite the pathogen on the agar plates

allowing the two fungi to confront each other. These confrontation plates were observed for any macroscopic differences between the wild type and mutants as each strain separately interaction with the hyphae of *R. solani* (Fig. 24). Although there is an obvious effect of the lack of Fe on the growth of the strains of *T. virens*, there is no obvious difference among the strains of *T. virens* in their interaction with *R. solani*. Enzymatic and biological control assays need to be performed to determine any large-scale effect of these gene disruptions.

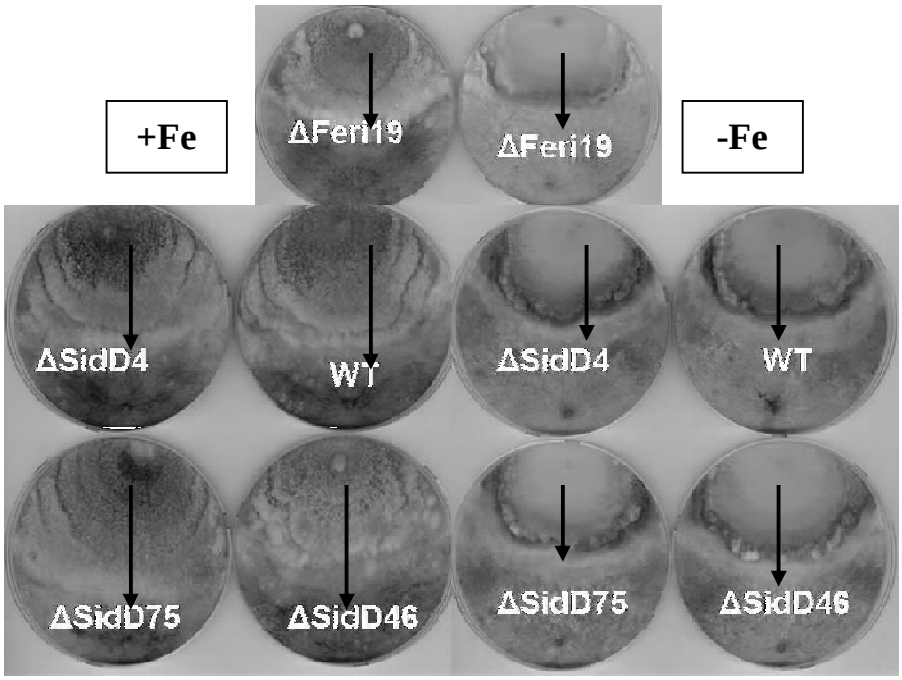

Fig. 24 Photos of Grimm-Allen agar plates showing *T. virens* confronted with *R. solani*. The left half were grown under high Fe while the right half were grown under Fe deprivation. Arrows indicate the length of the hyphal extension of *T. virens*.

The last phenotypic assay conducted was a test of the response of the strains to in vitro oxidative stress. Extracellular siderophore production has been linked to the ability to resist oxidative stress in other microbes (see experimental procedures section). Therefore, the *T. virens* strains were grown in the presence of hydrogen peroxide (H_2O_2) to observe if their growth was affected (Fig. 25). There is a significant difference between the wild type and the three Δ*Tex20* mutants when H_2O_2 was present in the medium at both two and three days of growth. The reduction in growth of the mutants is likely due to the fact that enzymes such as catalase that catabolize reactive oxygen species are rendered ineffective without Fe as a cofactor. When Fe levels inside the cell are reduced because the extracellular siderophores are not present or functioning properly (such as in these mutants), enzymes that require Fe to function normally will show lower activities.

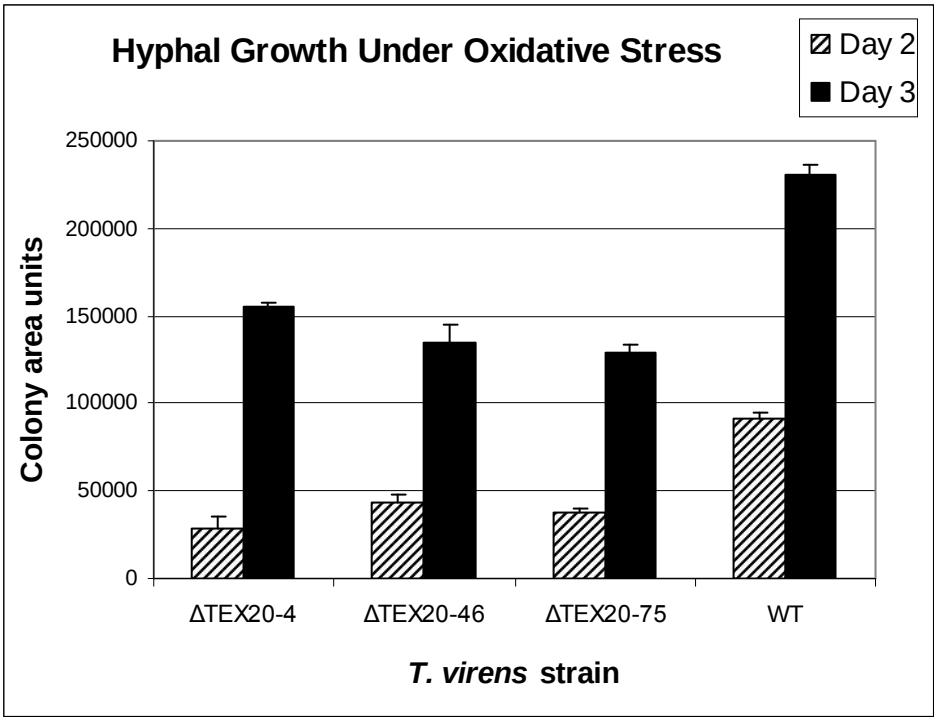

Fig. 25 Hyphal growth under oxidative stress. Oxidative stress response was tested by growing cultures on agar plates with 7 mM H_2O_2. Hyphal growth areas were measured at two and three days using ImageJ software. Standard error bars are shown for each data set. ANOVA indicates that each mutant is significantly different from the wild type with $p<0.0002$.

V CONCLUSIONS

The goal of this research was to determine the presence, regulation, production, and activity of siderophores in *Trichoderma virens*. Three genes which encode NRPSs that biosynthesize siderophores were found in the genome: *Tex20,* a homologue of SidD, likely encodes a NRPS that synthesizes the extracellular siderophore TAFC. *Tex10,* a homologue of NRPS2, likely encodes a NRPS that synthesizes the intracellular siderophore ferricrocin. *Tex21*, a homologue of NRPS6, likely produces a NRPS which synthesizes the extracellular siderophore coprogen. A gene disruption scheme was developed for *Tex21* and successful knockouts were generated for *Tex10* and *Tex20*. The gene expression profile for each of these genes was elucidated using RT-PCR. This showed that all three genes are most highly expressed after three days of growth in liquid medium without Fe. No *Tex10, Tex20,* or *Tex21* mRNA was produced when Fe was abundant in the medium. *Tex21* also showed expression at five days without Fe and *Tex10* was expressed at 5 and 7 days without Fe. The ΔTEX10-19 and ΔTEX20 mutants showed corresponding lack or reduction of mRNA. These data matched siderophore production levels revealed by HPLC. Thus, siderophore activity was measured from two levels: Tex gene expression and compound secretion. It appears that the NRPS encoded

by *Tex10* is producing a siderophore which is involved in basic life processes such as sporulation, spore germination, and hyphal growth as determined by comparison of the mutant and wild type in phenotypic assays. Additionally, the siderophore produced by the NRPS encoded by *Tex20* appears to be involved in oxidative stress response and to a small extent in spore germination.

Future studies are necessary to generate a successful knockout strain of *Tex21* using the procedure outlined here. Once this is accomplished, a double knockout strain in which both Tex 20 and 21 are disrupted would result in a mutant in which both putative extracellular siderophores are not synthesized or synthesized at such low levels as to be ineffective in iron acquisition. This strain would allow for confirmation that these genes are involved in siderophore production (by gene expression and HPLC analysis) and the role that siderophores play in any life process in *T. virens*, since it would likely show dramatic phenotypic deficiencies. Additionally, identification of the major siderophore peak at about 7 minutes in the chromatograms produced by the HPLC analysis is necessary. This can be done using MS/MS or MALDI-TOF MS. Additionally, it will be important to understand the impact of siderophores on mycoparasitism and induced resistance in *T. virens.* These are its most important

capabilities, and the double knockout strain could help to determine if siderophores are impacting them.

Trichoderma virens is a remarkable organism because it elicits systemic resistance in plants, mycoparasitizes pathogenic fungi, and enhances plant growth and development. Therefore, a better understanding of siderophores is necessary in this organism because Fe metabolism could be involved in any of these unique capabilities. If siderophore activity could be enhanced via the improvement of genes which encode NRPSs in *T. virens*, a more effective mycoparasite or elicitor fungus could result that would positively impact global agriculture.

REFERENCES

Baek, J. M. and Kenerley, C. M. (1998) The arg2 gene of *Trichoderma virens*: Cloning and development of a homologous transformation system. *Fungal Genetics and Biology,* **23,** 34-44.

Baker, B. J. and Banfield, J. F. (2003) Microbial communities in acid mine drainage. *FEMS Microbiology Ecology,* **44,** 139-152.

Chaudhuri, S. K., Lack, J. G. and Coates, J. D. (2001) Biogenic magnetite formation through anaerobic biooxidation of Fe(II). *Applied and Environmental Microbiology,* **67,** 2844-2848.

Djonovic, S., Pozo, M. J. and Kenerley, C. M. (2006) Tvbgn3, a beta-1,6-glucanase from the biocontrol fungus *Trichoderma virens,* is involved in mycoparasitism and control of Pythium ultimum. *Applied and Environmental Microbiology,* **72,** 7661-7670.

Djonovic, S., Vittone, G., Mendoza-Herrera, A., and Kenerley, C. M. (2007) Enhanced biocontrol activity of *Trichoderma virens* transformants constitutively coexpressing beta-1,3- and beta-1,6-glucanase genes. *Molecular Plant Pathology,* **8,** 469-480.

Finking, R. and Marahiel, M. A. (2004) Biosynthesis of nonribosomal peptides. *Annual Review of Microbiology,* **58,** 453-488.

Grunewald, J. and Marahiel, M. A. (2006) Chemoenzymatic and template-directed synthesis of bioactive macrocyclic peptides. *Microbiology and Molecular Biology Reviews,* **70,** 121-146.

Haas, H. (2003) Molecular genetics of fungal siderophore biosynthesis and uptake: the role of siderophores in iron uptake and storage. *Applied Microbiology and Biotechnology,* **62,** 316-330.

Harman, G. E., Howell, C. R., Viterbo, A., Chet, I. and Lorito, M. (2004) Trichoderma species - Opportunistic, avirulent plant symbionts. *Nature Reviews Microbiology,* **2,** 43-56.

Hissen, A. H. T., Chow, J. M. T., Pinto, L. J. and Moore, M. M. (2004) Survival of *Aspergillus fumigatus* in serum involves removal of iron from transferrin: the role of siderophores. *Infection and Immunity,* **72,** 1402-1408.

Jackson, A. M., Whipps, J. M. and Lynch, J. M. (1991) Nutritional studies of four fungi with disease biocontrol potential. *Enzyme and Microbial Technology,* **13,** 456-461.

Jalal, M. A. F., Love, S. K. and Vanderhelm, D. (1986) Siderophore Mediated Iron(III) Uptake In *Gliocladium virens* .1. Properties of Cis-Fusarinine, Trans-Fusarinine, Dimerum Acid, And Their Ferric Complexes. *Journal of Inorganic Biochemistry,* **28,** 417-430.

Jalal, M. A. F., Love, S. K. and Vanderhelm, D. (1987) Siderophore Mediated Iron(III) Uptake In *Gliocladium virens*. 2. Role of Ferric Monohydroxamates and Dihydroxamates as Iron Transport Agents. *Journal of Inorganic Biochemistry,* **29,** 259-267.

Jayaraj, J. and Radhakrishnan, N. V. (2008) Enhanced activity of introduced biocontrol agents in solarized soils and its implications on the integrated control of tomato damping-off caused by Pythium spp. *Plant and Soil,* **304,** 189-197.

Johnson, L. (2007) Iron and siderophores in fungal-host interactions. *Mycological Research,* **112,** 170-183.

Konetschny-Rapp, S., Huschka, Hans-Georg, Winkelmann, Gunther, & Jung, Gunther (1988) High-performance liquid chromatography of siderophores from fungi. *Biology of Metals,* 9-17.

Lee, B. N., Kroken, S., Chou, D. Y. T., Robbertse, B., Yoder, O. C. and Turgeon, B. G. (2005) Functional analysis of all nonribosomal peptide synthetases in *Cochliobolus heterostrophus* reveals a factor, NPS6, involved in virulence and resistance to oxidative stress. *Eukaryotic Cell,* **4,** 545-555.

Lewis, J. A., Larkin, R. P. and Rogers, D. L. (1998) A formulation of Trichoderma and Gliocladium to reduce damping-off caused by *Rhizoctonia solani* and saprophytic growth of the pathogen in soilless mix. *Plant Disease,* **82,** 501-506.

Llewellyn, N. M. and Spencer, J. B. (2007) Biological chemistry: Enzymes line up for assembly. *Nature,* **448,** 755-756.

Mercado-Blanco, J. and Bakker, P. (2007) Interactions between plants and beneficial Pseudomonas spp.: exploiting bacterial traits for crop protection. *Antonie Van Leeuwenhoek International Journal of General and Molecular Microbiology,* **92,** 367-389.

Miethke, M. and Marahiel, M. A. (2007) Siderophore-based iron acquisition and pathogen control. *Microbiology and Molecular Biology Reviews,* **71,** 413-451.

Neilands J., Schwyn B., Coy M., Francis R., and Paw B. (1987) *Iron transport in microbes, plants and animals.* . New York: VCH Weinheim.

Oide, S., Krasnoff, S. B., Gibson, D. M. and Turgeon, B. G. (2007) Intracellular siderophores are essential for ascomycete sexual development in heterothallic *Cochliobolus heterostrophus* and homothallic *Gibberella zeae*. *Eukaryotic Cell,* **6,** 1339-1353.

Oide, S., Moeder, W., Krasnoff, S., Gibson, D., Haas, H., Yoshioka, K., *et al.* (2006) NPS6, encoding a nonribosomal peptide synthetase involved in siderophore-mediated iron metabolism, is a conserved virulence determinant of plant pathogenic ascomycetes. *Plant Cell,* **18,** 2836-2853.

R.H. Garrett, C. M. G. (2005) *Biochemistry*. Belmont: Thomson Learning Brooks/Cole.

Reiber, K., Reeves, E. P., Neville, C. M., Winkler, R., Gebhardt, P., Kavanagh, K., *et al.* (2005) The expression of selected non-ribosornal peptide synthetases in *Aspergillus fumigatus* is controlled by the availability of free iron. *FEMS Microbiology Letters,* **248,** 83-91.

Sanderson, K. E. and Srb, A. M. (1965) Heterokaryosis And Parasexuality In Fungus *Ascochyta Imperfeceta*. *American Journal of Botany,* **52,** 72-&.

Schrettl, M., Bignell, E., Kragl, C., Sabiha, Y., Loss, O., Eisendle, M., *et al.* (2007) Distinct roles for intra- and extracellular siderophores during *Aspergillus fumigatus* infection. *PLOS Pathogens,* **3,** 1195-1207.

Schwecke, T., Gottling, K., Durek, P., Duenas, I., Kaufer, N. F., Zock-Emmenthal, S., *et al.* (2006) Nonribosomal peptide synthesis in *Schizosaccharomyces pombe* and the Architectures of ferrichrome-type siderophore synthetases in fungi. *Chembiochem,* **7,** 612-622.

Skoog, D. A., Holler, F.J., Crouch S.R. (2007) Principles of Instrumental Analysis. (ed.^eds.). Belmont: Thomson Brooks/Cole.

Stack, D., Neville, C. and Doyle, S. (2007) Nonribosomal peptide synthesis in *Aspergillus fumigatus* and other fungi. *Microbiology,* **153,** 1297-1306.

Tobiasen, C., Aahman, J., Ravnholt, K. S., Bjerrum, M. J., Grell, M. N. and Giese, H. (2007) Nonribosomal peptide synthetase (NPS) genes in *Fusarium graminearum, F-culmorum* and *F-pseudograminearium* and identification of NPS2 as the producer of ferricrocin. *Current Genetics,* **51,** 43-58.

Vinale, F., Sivasithamparam, K., Ghisalberti, E. L., Marra, R., Woo, S. L. and Lorito, M. (2008) Trichoderma-plant-pathogen interactions. *Soil Biology & Biochemistry,* **40,** 1-10.

Weber, K. A., Achenbach, L. A. and Coates, J. D. (2006) Microorganisms pumping iron: anaerobic microbial iron oxidation and reduction. *Nature Reviews Microbiology,* **4,** 752-764.

Wei, X. Y., Yang, F. Q. and Straney, D. C. (2005) Multiple non-ribosomal peptide synthetase genes determine peptaibol synthesis in *Trichoderma virens*. *Canadian Journal of Microbiology,* **51,** 423-429.

Welzel, K., Eisfeld, K., Antelo, L., Anke, T. and Anke, H. (2005) Characterization of the ferrichrome A biosynthetic gene cluster in the homobasidiomycete *Omphalotus olearius*. *FEMS Microbiology Letters,* **249,** 157-163.

Wiebe, M. G. (2002) Siderophore production by *Fusarium venenatum* A3/5. *Biochemical Society Transactions,* **30,** 696-698.

Wiest, A., Grzegorski, D., Xu, B. W., Goulard, C., Rebuffat, S., Ebbole, D. J., *et al.* (2002) Identification of peptaibols from *Trichoderma virens* and cloning of a peptaibol synthetase. *Journal of Biological Chemistry,* **277,** 20862-20868.

Wilhite, S. E., Lumsden, R. D. and Straney, D. C. (2001) Peptide synthetase gene in *Trichoderma virens*. *Applied and Environmental Microbiology,* **67,** 5055-5062.

Winkelmann, G. (2007) Ecology of siderophores with special reference to the fungi. *Biometals,* **20,** 379-392.

Yu, J. H., Hamari, Z., Han, K. H., Seo, J. A., Reyes-Dominguez, Y. and Scazzocchio, C. (2004) Double-joint PCR: a PCR-based molecular tool for gene manipulations in filamentous fungi. *Fungal Genetics and Biology,* **41,** 973-981.

APPENDIX

Fig. 1 was adapted with permission from *Mycological Research*, Volume 112, by Linda Johnson, Iron and Siderophores in Fungal-Host Interactions, pages 170-183, copyright 2008. Permission granted from Elsevier (Fig. 26) and from Linda Johnson (Fig. 27):

ELSEVIER LIMITED LICENSE TERMS AND CONDITIONS	
Apr 07, 2008	
This is a License Agreement between Gloria E. Vittone ("You") and Elsevier Limited ("Elsevier Limited"). The license consists of your order details, the terms and conditions provided by Elsevier Limited, and the payment terms and conditions.	
Supplier	Elsevier Limited The Boulevard,Langford Lane Kidlington,Oxford,OX5 1GB,UK
Registered Company Number	1982084
Customer name	Gloria E. Vittone
License Number	1923950401525
License date	Apr 07, 2008
Licensed content publisher	Elsevier Limited
Licensed content publication	Mycological Research
Licensed content title	Iron and siderophores in fungal–host interactions

Licensed content author	Johnson Linda
Licensed content date	February 2008
Volume number	112
Issue number	2
Pages	14
Type of Use	Thesis / Dissertation
Portion	Figures/table/illustration/abstracts
Portion Quantity	1
Format	Electronic
You are an author of the Elsevier article	No
Are you translating?	No
Purchase order number	
Expected publication date	May 2008
Elsevier VAT number	GB 494 6272 12

LIMITED LICENSE

Translation: This permission is granted for non-exclusive world **English** rights only unless your license was granted for translation rights. If you licensed translation rights you may only translate this content into the languages you requested. A professional translator must perform all translations and reproduce the content word for word preserving the integrity of the article. If this license is to re-use 1 or 2 figures then permission is granted for non-exclusive world rights in all languages.

Website: The following terms and conditions apply to electronic reserve and author websites:

your thesis be published commercially, please reapply for permission. These requirements include permission for the Library and Archives of Canada to supply single copies, on demand, of the complete thesis and include permission for UMI to supply single copies, on demand, of the complete thesis. Should your thesis be published commercially, please reapply for permission.

Fig. 26 Elsevier license.

Subject:RE: permission to use figure

Sent By: linda On:April 14, 2008 10:34 AM

To: "Gloria Elizabeth Vittone" <gigemglo2008@neo.tamu.edu>

Dear Gloria,

Yes you have my permission to use figure 1 in your thesis. Best of luck!

Kind Regards,

Linda Johnson

-----Original Message-----

From: Vittone, Gloria Elizabeth [mailto:gigemglo2008@neo.tamu.edu]

To: Johnson, Linda

Subject: permission to use figure

Dear Dr. Johnson,

My name is Gloria Vittone and I am writing an undergraduate thesis for the Honors Undergraduate Research Fellows program at Texas A&M Univeristy in the United States. I am hoping to use an adapted form of Figure 1 from your recent manuscript in the Journal of Mycological Research in the article "Iron and siderophores in fungal-host interactions." I have already obtained the license from elsevier in order to use this figure in my thesis, which will be published in the digital repository at Texas A&M Univeristy. I would also like your permission to use this figure in my thesis. Thank you very much.

Sincerely, Gloria Vittone

Fig. 27 Email correspondence.

CURRICULUM VITA

Gloria Vittone
Gigemglo2008@tamu.edu

EDUCATION

Texas A&M University

University Honors Program

Graduation with a B.S. May 10, 2008

Double major: Biochemistry & Genetics

Minor: Spanish

GPR 3.898

GRE general test: 1430

Baylor College of Medicine Interdepartmental Program in Cell and Molecular Biology Ph.D. program beginning August 2008

RESEARCH

Texas A&M 2008 University Honors Undergraduate Research Fellows Program

- Thesis: *Genetic and Functional Analysis of Siderophores in Trichoderma virens*

- Lab research with Dr. Charles Kenerley, Department of Plant Pathology & Microbiology: generate two knock-out strains in *T. virens* to elucidate the role of siderophores
- Oral Research presentations: October 2007, February 2008, April 2008
- Student Research Week poster presentation, spring 2008
- Skills: protein purification and analysis, gene knock-out via homologous recombination, PCR, microbial culture, primer design, DNA/RNA extraction, microscopy, spectroscopy, RT-PCR, HPLC

Texas A&M University Department of Plant Pathology, College Station, TX

- Undergraduate research assistant in Dr. Charles Kenerley's laboratory
- Collaborate with Dr. Slavica Djonovic on experiments involving systemic induced resistance and biological control
- Second author: *Enhanced biocontrol activity of Trichoderma virens transformants constitutively coexpressing β-1,3- and β-1,6-glucanase genes*. Molecular Plant Pathology: 8(4), 2007.

Texas A&M University, Department of Biochemistry & Biophysics, College Station, TX

- Laboratory technician, Dr. James Hu's laboratory

- Laboratory maintenance: media and supply preparation and clean-up

INTERNATIONAL EXPERIENCE

Español en Toledo (ESTO) program, Texas A&M University

- Live with host family in Toledo, Spain for summer 2005
- Universidad de Castilla la Mancha, completed 6 hours of Spanish courses

ACTIVTES, AWARDS, & HONORS

- Graduation with University Honors and Suma Cum Laude, May 2008
- Summer University Undergraduate Research Fellows Scholarship, May 2007
- Texas A&M University President's Endowed Scholarship, May 2004
- 2008 Texas A&M Student Research Week Session Winner (Molecular Biology), 1st Place in Molecular Biology Taxonomy, and Winner of the Interdisciplinary Research Award.
- Phi Lambda Upsilon, chemistry honor society, January 2007
- Phi Kappa Phi, national academic honor society, January 2006
- Big Sister: Big Brothers & Big Sisters of North America, November 2006
- Texas A&M University Cancer Society, January 2005
- English Language Institute conversation partner, August 2005